PIKfyve/Fab1 is required for efficient V-ATPase delivery to phagosomes, phagosomal killing, and restriction of *Legionella* infection

Catherine M. Buckley[1,2], Victoria L. Heath[3], Aurélie Guého[4], Stephen K. Dove[5], Robert H. Michell[5], Roger Meier[6#], Hubert Hilbi[7], Thierry Soldati[4], Robert H. Insall[8*] and Jason S. King[1,2*]

[1] Centre for Membrane Interactions and Dynamics, Department of Biomedical Sciences, University of Sheffield, Firth Court, Western Bank, Sheffield. S10 2TN, UK

[2]Bateson Centre, University of Sheffield, Firth Court, Western Bank, Sheffield. S10 2TN, UK

[3]Institute of Cardiovascular Sciences, Institute for Biomedical Research, College of Medical and Dental Sciences, University of Birmingham, Edgbaston, Birmingham, B15 2TT, UK

[4]Department of Biochemistry, Faculty of Sciences, University of Geneva, CH-1211 Geneva, Switzerland

[5]School of Biosciences, University of Birmingham, Edgbaston, Birmingham. B15 2TT, UK

[6]Institute of Molecular Life Sciences, University of Zürich, CH-8057 Zürich, Switzerland

[7]Institute of Medical Microbiology, University of Zürich, CH-8006 Zürich, Switzerland

[8]CRUK Beatson Institute, Switchback Road, Bearsden, Glasgow G61 1BD, UK

[#]Present address: Scientific Center for Optical and Electron Microscopy, ETH Zürich, CH-8093 Zürich, Switzerland

[*]To whom correspondence should be addressed:

Jason.King@sheffield.ac.uk

R.Insall@beatson.gla.ac.uk

Abstract

By engulfing potentially harmful microbes, professional phagocytes are continually at risk from intracellular pathogens. To avoid becoming infected, the host must kill pathogens within the phagosome before they can escape or establish a survival niche. Here, we analyse the role of the phosphoinositide (PI) 5-kinase PIKfyve in phagosome maturation and killing, using the amoeba and model phagocyte *Dictyostelium discoideum*.

By binding to phosphatidylinositol-3-phosphate (PI3P) and phosphorylating it to PI(3,5)P_2, PIKfyve plays important, but poorly understood, roles in vesicular trafficking. Here we show that PIKfyve activity is essential during early phagosome maturation. Disruption of *PIKfyve* inhibited delivery of the vacuolar V-ATPase, dramatically reduced the ability of *Dictyostelium* cells to acidify newly-formed phagosomes. Consequently, *PIKfyve*-null cells were unable to digest phagosomal contents and generate an effective antimicrobial environment. PI(3,5)P_2 is therefore essential for phagocytes to efficiently kill captured bacteria and we demonstrate that cells lacking *PIKfyve* are more susceptible to infection by the intracellular pathogen *Legionella pneumophila.* We conclude that PIKfyve-catalysed PI(3,5)P_2 production plays a crucial and general role in ensuring early phagosomal maturation, thus protecting host cells from diverse pathogenic microbes.

Author summary

Cells that capture or eat bacteria must swiftly kill them to prevent potential pathogens surviving long enough to escape and establish an infection. This is achieved by the rapid delivery of components that produce an antimicrobial environment in the phagosome, the compartment containing the captured microbe. This is essential both for the function of immune cells and for amoebae that feed on bacteria in their environment. Here, we identify a new signalling pathway that regulates the delivery of antimicrobial components to the phagosome, and show that bacteria survive over three times as long within the host if this pathway is disabled. We show that this is of general importance for killing a wide range of pathogenic and non-pathogenic bacteria, and that it is physiologically important for cells to prevent infection by the opportunistic human pathogen *Legionella*.

Introduction

It is essential for professional phagocytes to kill their prey rapidly and efficiently to prevent the establishment of infections and disease. Multiple mechanisms are employed to achieve this and once phagosomes have been internalised they quickly become acidified and acquire reactive oxygen species, antimicrobial peptides and acid hydrolases. The timely and regulated delivery of these components is vital to protect the host from intracellular pathogens, but is incompletely understood.

After the phagosome is internalised, specific effector proteins are recruited to its cytoplasmic surface by interacting with several inositol phospholipids (PIPs) that play important roles in regulating vesicle trafficking and controlling maturation. The effectors of each PIP regulate particular aspects of compartment identity, membrane trafficking and endosomal maturation [1, 2]. Phosphatidylinositol-3-phosphate (PI(3)P), made by the class III PI 3-kinase VPS34, is one of the first PIPs to accumulate on vesicles after endocytosis, and it recruits proteins containing FYVE (Fab1, YOTB, Vac1 and EEA1) and PX domains – including, respectively, the characteristic early endosome markers EEA1 and Hrs, and sorting nexins [3, 4]. Also recruited to early endosomes by its FYVE domain is PIKfyve (known as Fab1 in yeast) [5], a phosphoinositide 5-kinase that phosphorylates PI(3)P to phosphatidylinositol-3,5-bisphosphate (PI(3,5)P_2) [6-10]. The roles of PI(3)P are well explored, but the formation of PI(3,5)P_2 and the identities and functions of its various effector proteins are less well understood [11-13]. PI(3,5)P_2 is thought to accumulate predominantly on late endosomes, and disruption of PIKfyve activity leads to multiple endocytic defects, including gross endosomal enlargement and accumulation of autophagosomes [14-19]. Recent research has begun to reveal important physiological roles of PIKfyve in a range of cell types and animals although mechanistic details remain sparse [20-24].

Like classical endocytosis, phagosome maturation is regulated by PIPs [25]. Phagosomes accumulate PI(3)P immediately after closure, and this is required for their subsequent maturation [26-28]. The recent identification of several PIKfyve inhibitors, including apilimod and YM201636 [29, 30], has allowed researchers to demonstrate the importance of PI(3)P to PI(3,5)P_2 conversion for phagosomal maturation in macrophages [31, 32]. However, there are conflicting reports on the roles of PIKfyve during key maturation steps such as acidification and degradation of bacteria, and its functional role remains subject to much debate.

To understand the function and physiological significance of PIKfyve, we have investigated its role in phagosome maturation and pathogen killing in the model organism *Dictyostelium discoideum,* a soil-dwelling amoeba and professional phagocyte that feeds on bacteria. *Dictyostelium* PIPs are unusual, with the lipid chain joined to the *sn*-1-position of the glycerol backbone by an ether, rather than

82 ester, linkage: these PIPs should correctly be named as derivatives of plasmanylinositol rather than
83 phosphatidylinositol [33]. This however, appears to make no difference to downstream functions,
84 which are dictated by interactions with the inositol polyphosphate headgroup. *Dictyostelium* has
85 thus been an effective model for analysis of phosphoinositide signalling [34-37]. For convenience,
86 both the mammalian and *Dictyostelium* inositol phospholipids are referees to as PIPs hereafter.

87 We find that genetic or pharmacological disruption of PIKfyve activity in *Dictyostelium* leads to a
88 swollen endosomal phenotype reminiscent of defects in macrophages, and we provide a detailed
89 analysis of phagosome maturation. We show that at least some of the defects in PIKfyve-deficient
90 phagosome maturation are due to reduced recruitment of the proton-pumping vacuolar (V-ATPase).
91 Furthermore, we provide the first demonstration that PIKfyve is required for the efficient killing of
92 phagocytosed bacteria and for restricting the intracellular growth of the pathogen *Legionella*
93 *pneumophila.*

94

95 ## Results

96 ***PIKfyve*- null cells have swollen endosomes**

97 The *Dictyostelium* genome contains a single orthologue of *PIKfyve* (*PIP5K3*). Like the mammalian and
98 yeast proteins, *Dictyostelium* PIKfyve contains an N-terminal FYVE domain, a CCT (chaperonin
99 Cpn60/TCP1)-like chaperone domain, a PIKfyve-unique cysteine/histidine-rich domain and a C-
100 terminal PIP kinase domain [6]. In order to investigate the role of PI(3,5)P_2 in *Dictyostelium* we
101 disrupted the *PIKfyve* gene by inserting a blasticidin resistance cassette and deleting a portion of the
102 central PIKfyve-unique region (Supplementary Figure 1). To control for differences in genetic
103 backgrounds, mutants were generated in both Ax3 and Ax2 axenic strains.

104 While the unusual ether-linked chemistry of the *Dictyostelium* inositol phospholipids prevented
105 direct measurement of PI(3,5)P_2 loss by either the standard method of methanolysis followed by
106 HPLC of deacylation products or mass spectrometry (P.T. Hawkins, personal communication), we
107 found that each mutant strain was highly vacuolated (Figure 1A and B), resembling the swollen
108 vesicle phenotype observed upon *PIKfyve* knockdown or inhibition in mammalian cells, *C. elegans*, *S.*
109 *cerevisiae* and *D. melanogaster* [9, 14, 19, 38]. Identical results were also obtained with *PIKfyve*- cells
110 generated in an Ax2 background and this effect was phenocopied by incubation with the PIKfyve-
111 specific inhibitor apilimod [29], confirming that this phenotype was due to deficient PI(3,5)P_2
112 synthesis (Figure 1C).

113 When amoebae were hypotonically stressed in phosphate buffer, we observed a sustained increase
114 in vacuolation for at least 5 hours. However, after 24 hours, when the cells became polarized
115 (indicating the onset of starvation-induced development), *PIKfyve*- mutants became
116 indistinguishable from the random integrant and parental controls (Figure 1B). This is most likely due
117 to the well-documented suppression of fluid-phase uptake that occurs when *Dictyostelium* cells
118 enter starvation-induced development [39, 40]. Consistent with this, *PIKfyve* null cells had no
119 observable delay or other defects in development, and formed morphologically normal fruiting
120 bodies with viable spores (Supplementary figure 2). Disruption of PI(3,5)P_2 synthesis therefore leads
121 to endocytic defects, but it is not required for *Dictyostelium* development.

122 When amoebae were hypotonically stressed in phosphate buffer, we observed a sustained increase
123 in vacuolation for at least 5 hours. However, after 24 hours, when the cells became polarized
124 (indicating the onset of starvation-induced development), *PIKfyve*$^-$ mutants became
125 indistinguishable from the random integrant and parental controls (Figure 1B). This is most likely due
126 to the well-documented suppression of fluid-phase uptake that occurs when *Dictyostelium* cells
127 enter starvation-induced development [39, 40]. Consistent with this, *PIKfyve*-null cells showed no

128 observable delay or other defects in development, and formed morphologically normal fruiting
129 bodies with viable spores (Supplementary Figure 2). We conclude that loss of PIKfyve activity
130 therefore leads to endocytic defects, but it is not required for *Dictyostelium* development.

131 **PIKfyve is important for phagocytic growth but not uptake**

132 Laboratory strains of *Dictyostelium* can obtain nutrients either by macropinocytosis of liquid (axenic)
133 medium or by phagocytosis of bacteria. Whilst *PIKfyve*- null cells had normal rates of endocytosis
134 and exocytosis, axenic growth was slower than for wild-type cells, with mutants doubling every 16
135 hours compared to 10 hours for the controls (Figure 2A-C)..

136 In contrast, growth on bacteria was more strongly affected, and *PIKfyve* null cells formed much
137 smaller colonies on lawns of avirulent *Klebsiella pneumoniae* (Figure 2D). To confirm this defect and
138 test its generality, we screened *PIKfyve*-null cells for growth on a palette of diverse Gram-positive
139 and Gram-negative bacteria, including both pathogenic and non-pathogenic strains. PIKfyve was
140 required for efficient growth in all cases, indicating a general role for PI(3,5)P_2 synthesis for
141 phagocytic growth (Figure 2E and F).

142 Defective growth on bacteria could be due to disruption of either capture, killing or digestion. To
143 measure if phagocytic uptake was affected by PIKfyve disruption, we monitored the ability of
144 *Dictyostelium* cells to reduce the turbidity of an *E. coli* suspension over time (Figure 3A). No
145 difference was observed in the ability of *PIKfyve* null cells to phagocytose bacteria compared to the
146 parental strain. To confirm this, we also measured phagocytosis of fluorescent beads (Figure 3B) and
147 GFP-expressing *Mycobacterium smegmatis* (Figure 3C) by flow cytometry and found no defect in
148 uptake by *PIKfyve* null cells. As bacteria are efficiently captured, PIKfyve must therefore be
149 important for phagosome processing.

150 **PIKfyve does not regulate PI(3)P dynamics in *Dictyostelium***

151 PI(3)P is one of the best characterized early markers of maturing endosomes and phagosomes. In
152 both mammalian macrophages and in *Dictyostelium.* Immediately following particle internalization,
153 PI(3)P is generated on the phagosome by the class III PI 3-kinase VPS34 [26, 32, 41] and interacts
154 with a number of important regulators of maturation such as Rab5 [42]. PIKfyve is both recruited by
155 PI(3)P and phosphorylates it, forming PI(3,5)P_2. Absence of *PIKfyve* could perturb phagosome
156 maturation by reducing PI(3)P consumption, by eliminating the actions of PI(3,5)P_2, or both. Indeed,
157 studies in macrophages indicate that inhibition of PIKfyve can cause prolonged PI(3)P signalling [32].

158 We therefore investigated the contribution of PIKfyve to PI(3)P dynamics in *Dictyostelium*. PI(3)P can
159 be visualized in cells using the well-characterised reporter GFP-2xFYVE [34, 43]. Expression of GFP-
160 2xFYVE in control cells demonstrated PI(3)P is present on *Dictyostelium* phagosomes following
161 engulfment, consistent with previous reports [41] (Figure 4A). However, we found defects in neither
162 initial recruitment, nor dissociation of this reporter in *PIKfyve* mutants (Figure 4A and B). Therefore,
163 PIKfyve activity does not significantly contribute to PI(3)P turnover in these cells. The defects in
164 growth, and the swollen endosomes are thus due to lack of PI(3,5)P_2 synthesis rather than prolonged
165 accumulation of PI(3)P.

166 ***PIKfyve* deficient phagosomes have defective acidification and digestion**

167 Next we investigated how absence of PIKfyve affects phagosomal maturation. One of the first stages
168 of maturation is the acquisition of the proton-pumping V-ATPase, leading to rapid acidification [44].
169 The influence of PIKfyve on endosomal pH regulation, however, remains controversial. Whilst
170 studies in *C. elegans,* plants and mammalian epithelial cells have shown that PIKfyve is required for
171 efficient acidification [38, 45-48], others have shown that RAW 264.7 macrophages are still able to
172 acidify their phagosomes to at least pH 5.5 when PIKfyve is inhibited [32].

173 We therefore assessed the ability of *Dictystelium PIKfyve*-null cells to acidify their phagosomes by
174 measuring the relative fluorescence of beads labelled with both the pH-sensitive FITC and the pH-
175 insensitive Alexa 594 succinimidyl ester [49]. The phagosomes of *PIKfyve*-null cells acidified much
176 more slowly than wild-type cells and never achieved as low a pH as those of wild-type cells (Figure
177 4C).

178 Proper degradation of internalised material requires both acidification and the presence of
179 proteases. We measured phagosomal proteolysis by following the increase in fluorescence due to
180 the cleavage and unquenching of DQ-BSA coupled to beads [49] (Figure 4D). Strikingly, phagosomes
181 of *PIKfyve*-null cells exhibited an almost complete loss of proteolytic activity, likely due to a
182 combination of delayed delivery of hydrolytic enzymes and their lower activity in inadequately
183 acidified phagosomes.

184 Phagosomal acidification is driven by the rapid recruitment and activity of the V-ATPase. The V-
185 ATPase consists of V_0 (transmembrane) and V_1 (peripheral) sub-complexes. It has previously been
186 shown that PI(3,5)P_2 can regulate V_0-V_1 assembly at the yeast vacuole allowing dynamic regulation of
187 activity [50]. To differentiate between defective V-ATPase delivery and assembly we expressed GFP-
188 fusions of both V_0 and V_1 subunits (GFP-VatM and VatB-GFP respectively) and observed their
189 recruitment to nascent phagosomes by fluorescence microscopy [51]. Both proteins were expressed

190 equally in wild-type and mutant cells (Supplementary figure 3) and by observing phagocytosis of pH-
191 sensitive pHrodo-labelled yeast we were also able to simultaneously monitor acidification.

192 Both GFP-VatM and VatB-GFP began accumulating on phagosomes immediately following
193 internalisation both in *PIKfyve*$^-$ and control cells, but the rate of accumulation was substantially
194 reduced in the mutants and only reached about half of the final levels observed in wild-type cells
195 (Figure 5A-D). Defective acidification was again demonstrated by a reduced increase in pHrodo
196 fluorescence (Figure 5E). It should be noted that expression of VatB-GFP (but not GFP-VatM) caused
197 a partial, but dominant, inhibition of acidification in this assay (Supplementary Figure 3A). The
198 observation that both V-ATPase components were equally affected indicates that PIKfyve is required
199 for delivery of the entire V-ATPase to the phagosome, rather than specifically affecting V_0-V_1
200 association.

201 **PIKfyve is essential for efficient killing of bacteria**

202 Acidification and proteolysis are important mechanisms used by phagocytes to kill engulfed
203 microbes. We therefore asked whether PIKfyve was physiologically important for killing. Bacterial
204 death leads to membrane permeabilisation and intracellular acidification, so survival time within
205 phagosomes can be inferred by observing the phagocytosis and subsequent quenching of GFP
206 expressed by a non-pathogenic *Klebsiella pneumoniae* strain [52]. In this assay, the phagocytised
207 bacteria survived for more than three times longer in *PIKfyve*$^-$ cells (median survival 12 min) than in
208 wild-type cells (3.5 min) (Figure 6A and B). These benign bacteria did however eventually die in
209 *PIKfyve* null cells, indicating either that the residual acidification is eventually sufficient, or other
210 elements of the complex bacterial killing machinery remain functional in the *PIKfyve*$^-$ phagosomes.

211 **PIKfyve activity restricts the persistence of *Legionella* infection**

212 Many pathogenic bacteria infect host immune cells by manipulating phagosome maturation to
213 establish a replication-permissive niche or to escape into the cytosol. To avoid such infection, host
214 cells must kill such pathogens rapidly. PIKfyve may therefore be critical to protect host cells from
215 infections.

216 *Legionella pneumophila* is a Gram-negative opportunistic human pathogen that normally lives in the
217 environment by establishing replicative niches inside amoebae such as *Acanthamoeba.* This process
218 can be replicated in the laboratory using *Dictyostelium* as an experimental host [53]. Following its
219 phagocytosis, *Legionella* can disrupt normal phagosomal maturation and form a unique *Legionella*-
220 containing vacuole (LCV). This requires the Icm/Dot (Intracellular multiplication/defective for

221 organelle trafficking) type IV secretion system that delivers a large number of bacterial effector
222 proteins into the host (reviewed in [54]). These effectors modify many host signalling and trafficking
223 pathways, one of which is to prevent the nascent *Legionella* phagosome from fusing with lysosomes
224 [55].

225 Phosphoinositide signalling is heavily implicated in *Legionella* pathogenesis. *Legionella*-containing
226 phagosomes rapidly accumulate PI(3)P. Its concentration then declines within 2 hours and PI(4)P
227 accumulates [56], and some of the effectors introduced through the Icm/Dot system bind PI(3)P or
228 PI(4)P [57-63]. The role of PI(3,5)P_2 in *Legionella* infection however is yet to be investigated. We
229 therefore tested whether PIKfyve was beneficial, or detrimental for the host to control *Legionella*
230 infection.

231 When we monitored the initial phase of infection, we found that both parental and *PIKfyve*$^-$
232 *Dictyostelium* phagocytised many more of the virulent wild-type *L. pneumophila* strain (JR32) than
233 an avirulent strain that is defective in type IV secretion (*ΔicmT*) [64] (Figure 7A). These results are in
234 agreement with the previous finding that expression of the Icm/Dot T4SS promotes uptake of *L.*
235 *pneumophila* [65]. To compensate for this difference in bacterial uptake, subsequent experiments
236 employed a multiplicity of infection (MOI) of 100 for the *ΔicmT* strain, and an MOI of 1 for the wild-
237 type JR32.

238 We next investigated whether *L. pneumophila* continue to multiply in, or are killed by, their
239 *Dictyostelium* hosts over several days. When viable bacteria released from the infected cells were
240 measured, both parental and *PIKfyve*$^-$ *Dictyostelium* almost eliminated the burden of avirulent *ΔicmT*
241 *Legionella* during the 6 days following infection (Fig 7B, note that the CFUs scales in Figs. 7B and 7C
242 are logarithmic). This was confirmed by observing a similar decline in the number of viable
243 intracellular bacteria that were released when the amoebae were lysed (Figure 7C).

244 However, the results with wild-type *Legionella* were very different: many more survived in *PIKfyve*$^-$
245 than in wild-type amoebae (Figure 7C) and were released into the medium in larger numbers (Figure
246 7B). Further confirmation of the enhanced survival of *Legionella* in *PIKfyve*$^-$ amoebae was obtained
247 by flow cytometric analysis of the bacterial load within *Dictyostelium* cells infected with GFP-
248 expressing *Legionella* (either wild-type or *ΔicmT*). The only *Dictyostelium* cells that accumulated
249 substantial GFP fluorescent over several days were those infected by wild-type *Legionella*, and this
250 happened sooner and to a greater degree in the *PIKfyve*-null cells (Figure 7D, central panels).

251

252 Manipulation of PIKfyve-mediated signalling is therefore not required for *L. pneumophila* to pervert
253 phagosome maturation and replicate intracellularly. Rather, the role of PIKfyve in ensuring rapid
254 phagosomal acidification and digestion is crucial to prevent *Legionella*, and presumably other
255 pathogens, from surviving and establishing a permissive niche.

256

257 ## Discussion

258 In this study, we have characterised the role of PIKfyve during phagosome maturation using the
259 model phagocyte *D. discoideum.* The roles of PI 3-kinases and PI(3)P signalling during phagosome
260 formation and early maturation have been studied extensively, but the subsequent actions of
261 PIKfvye and roles of PI(3,5)P_2 and PI(5)P are less well understood [2, 25]. In non-phagocytic cells such
262 as fibroblasts and yeast, PI(3,5)P_2 production is important for endosomal fission and fragmentation
263 of endolysosomal compartments [9, 17, 38, 46]. PIKfyve has also been shown to regulate
264 macropinosome maturation, and be functionally important for intracellular replication of both the
265 Vaccinia virus and *Salmonella* [47, 66, 67]. In this paper we show that PIKfyve is critical to ensure
266 efficient phagosomal acidification and proteolysis, and demonstrate its physiological importance in
267 the killing of bacteria and in suppression of intracellular pathogen survival.

268 Complex effects of PIKfyve inhibition on PIP-mediated signalling have hampered clear interpretation
269 of PIKfyve function in some mammalian studies. For example, some studies report that disruption of
270 PIKfyve prolonged PI(3)P-mediated signalling in addition to lack of PI(3,5)P_2 production [29, 31],
271 making it difficult to determine which phosphoinositide change is responsible for the observed
272 phenotypes. However, in agreement with other reports [17, 46], we found that deletion of PIKfyve
273 had no impact on phagosomal PI(3)P dynamics in *Dictyostelium*. The observed defects in phagosome
274 maturation appear therefore to be due to lack of PI(3,5)P_2 formation and not prolonged PI(3)P
275 signalling in this system.

276 The role of PIKfyve in lysosomal acidification and degradation is currently disputed. Several studies
277 which have measured vesicular pH at a single time point have shown that PIKfyve is required for
278 acidification [9, 38, 46, 48], but others found that disruption of PIKfyve had little effect on
279 phagosomal pH [32, 67, 68]. In contrast, we followed the temporal dynamics of V-ATPase delivery
280 and of phagosomal acidification and proteolysis, and showed that V-ATPase delivery to PIKfyve-
281 deficient phagosomes was substantially decreased and delayed, with consequent defects on initial
282 acidification and proteolysis. PI(3,5)P_2 has also been proposed to regulate V-ATPase V_0-V_1
283 subcomplex association dynamically at the yeast vacuole [50], but we found no evidence for this
284 during *Dictyostelium* phagosome maturation.

285 It is still not clear how PIKfyve-generated PI(3,5)P_2 regulates V-ATPase trafficking, and few PI(3,5)P_2
286 effectors are known. One of these is the lysosomal cation channel TRPML1/mucolipin, which is
287 specifically activated by PI(3,5)P_2 [69]. This interaction was recently shown to underlie the role of
288 PIKfyve in macropinosome fragmentation, although not acidification [67], and TRPML1 is also
289 required for phagosome-lysosome fusion [70]. Additionally, PI(3,5)P_2 and TRPML1 have been

290 proposed to mediate interactions between lysosomes and microtubules [71]. Therefore PIKfyve may
291 drive V-ATPase delivery to phagosomes by both microtubule-directed trafficking and by regulating
292 fission. However the sole mucolipin orthologue in *Dictyostelium* is only recruited to phagosomes
293 much later, during their post-lysosomal phase, and its disruption influences exocytosis rather than
294 acidification [72].

295 Rapid phagosomal acidification and proteolysis is key for phagocytes to kill internalised bacteria.
296 Many clinically relevant opportunistic pathogens, such as *L. pneumophila* [54, 73], *Burkholderia*
297 *cenocepacia* [74] and *Cryptococcus neoformans* [75] have developed the ability to subvert normal
298 phagosome maturation in order to maintain a permissive niche inside host phagocytes. This is likely
299 to have evolved from interactions with their environmental predators such as amoebae [76-78].

300 *L. pneumophila* are phagocytosed in the lung by alveolar macrophages, and after internalisation
301 employ effectors secreted via its type IV secretion system, some of which interfere with PI(3)P-
302 signalling, to inhibit phagosome maturation [58, 79, 80]. We have shown that the lipid products of
303 PIKfyve are not required for *L. pneumophila* to establish an intracellular replication niche. Rather, *L.*
304 *pneumophila* survive much better in PIKfyve-deficient cells, suggesting that PI(3,5)P_2 helps
305 *Dictyostelium* to eliminate, rather than harbour, *Legionella*. This is in contrast to the non-phagocytic
306 invasion of epithelia that occurs during *Salmonella* infection when PIKfyve activity is necessary to
307 promote the generation of a specialised survival niche within which the bacteria replicate [47].
308 *Salmonella* has therefore evolved a specialised role for the products of PIKfyve in generating a
309 survival niche, whereas *Legionella* and other bacteria are suppressed by PIKfyve-driven rapid
310 phagosomal maturation.

311 The molecular arms race between host and pathogens is complex and hugely important. The very
312 early events of phagosome maturation are critical in this competition; host cells aim to kill their prey
313 swiftly whilst pathogens try to survive long enough to escape. Although its molecular effectors
314 remain unclear, PIKfyve and its products are crucial to tip the balance in favour of the host, providing
315 a general mechanism to ensure efficient antimicrobial activity.

316 ## Materials and Methods

317 ### Cell strains and culture

318 *Dictyostelium discoideum* cells were grown in adherent culture in plastic Petri dishes in HL5 medium
319 (Formedium) at 22°C. *PIKfyve* null mutants were generated in both Ax2 and Ax3 backgrounds, with
320 appropriate wild-type controls used in each case. Cells were transformed by electroporation and
321 transformants selected in 20 µg/ml hygromycin (Invitrogen) or 10 µg/ml G418 (Sigma). Apilimod was
322 from United States Biological.

323 Growth in liquid culture was measured by seeding log phase cells in a 6 well plate and counting cells
324 every 12 hours using a haemocytometer. Growth on bacteria was determined by plating ~10
325 *Dictyostelium* cells on SM agar plates (Formedium) spread with a lawn of *K. pneumophila*.

326 Plaque assays were performed as previously described [81]. Briefly, serial dilution of *Dictyostelium*
327 cells (10-10^4) were placed on bacterial lawns and grown until visible colonies were obtained. The
328 bacterial strains were kindly provided by Pierre Cosson and were: *K. pneumoniae* laboratory strain
329 and 52145 isogenic mutant (Benghezal et al., 2006), the isogenic *P. aeruginosa* strains PT5 and
330 PT531 (*rhlR-lasR* avirulent mutant) (Cosson et al., 2002), *E.coli* DH5α (Fisher Scientific), *E. coli* B/r
331 (Gerisch, 1959), non-sporulating *B. subtilis* 36.1 (Ratner and Newell, 1978), and *M. luteus*
332 (Wilczynska and Fisher, 1994). An avirulent strain of *K. pneumophila* was obtained from ATCC (Strain
333 no. 51697).

334 The *Dictyostelium* development was performed by spreading 10^7 amoebae on nitrocellulose filters
335 (47 mm Millipore) on top of absorbent discs pre-soaked in KK2 (0.1 M potassium phosphate pH 6.1)
336 and images were taken at 20 hours [82].

337 ### Gene disruption and molecular biology

338 *PIKfyve* null cells in an Ax2 background were generated by gene disruption using homologous
339 recombination. A blasticidin knockout cassette was made by amplifying a 5' flanking sequence of the
340 *PIKfyve* gene (DDB_G0279149) (primers: fw- GGTAGATGTTTAGGTGGTGAAGT, rv-
341 gatagctctgcctactgaagCGAGTGGTGGAATTCATAAAGG) and 3' flanking sequence (primers: fw-
342 ctactggagtatccaagctgCCATTCAAGATAGACCAACCAATAG, rv- AGAATCAGAATAAACATCACCACC). These
343 primers contained cross over sequences (in lower case) allowing a LoxP-flanked blasticidin resistance
344 cassette (from pDM1079, a kind gift from Douwe Veltman) to be inserted between the two arms.

345 For *PIKfyve* gene disruption in an Ax3 background a knockout cassette was constructed in
346 pBluescript by sequentially cloning fragment I (amplified by
347 TAGTAGGAGCTCGGATCCGGTAGATGTTTAGGTGGTGAAGTTTTACCAAC and

348 TAGTAGTCTAGACGAGTGGTGGAATTCATAAAGGTACGTTCAT) and fragment II (amplified by
349 TAGTAGAAGCTTCCATTCAAGATAGACCAACCAATAGTAGTCCTGC and
350 TAGTAGGGTACCGGATCCCAGTGTGTAAATGAGAATCAGAATAAACATCACC). The blasticidin resistance
351 gene was inserted between fragment I and II as a XbaI – HindIII fragment derived from pBSRδBam
352 [83]. Both constructs were linearised, electroporated into cells and colonies were screened by PCR.
353 GFP-2xFYVE was expressed using pJSK489 [34], GFP-PH_{CRAC} with pDM631 [84] and GFP-VatM and
354 VatB-GFP with pMJC25 and pMJC31, respectively [85].

355 Microscopy and image analysis

356 Fluorescence microscopy was performed on a Perkin-Elmer Ultraview VoX spinning disk confocal
357 microscope running on an Olympus 1x81 body with an UplanSApo 60x oil immersion objective (NA
358 1.4). Images were captured on a Hamamatsu C9100-50 EM-CCD camera using Volocity software by
359 illuminating cells with 488 nm and 594 nm laser lines. Quantification was performed using Image J
360 (https://imagej.nih.gov).

361 To image PI(3)P dynamics, cells were incubated in HL5 medium at 4 °C for 5 mins before addition of
362 10 µl of washed 3 µm latex beads (Sigma) and centrifugation at 280 x *g* for 10 seconds in glass-
363 bottomed dishes (Mat-Tek). Dishes were removed from ice and incubated at room temperature for
364 5 mins before imaging. Images were taken every 30 s across 3 fields of view for up to 30 mins.

365 V-ATPase recruitment and acidification was performed using *Saccharomyces cerevisiae* labelled with
366 pHrodo red (Life Technologies) as per the manufacturers instructions. *Dictyostelium* cells in HL5
367 medium were incubated with $1x10^7$ yeast per 3 cm dish, and allowed to settle for 10 mins before the
368 medium was removed and cells were gently compressed under a 1% agarose/HL5 disk. Images were
369 taken every 10 s across 3 fields of view for up to 20 mins. Yeast particles were identified using the
370 "analyse particles" plugin and mean fluorescence measured over time. V-ATPase recruitment was
371 measured as the mean fluorescence within a 0.5 µm wide ring selection around the yeast. The signal
372 was then normalised to the initial fluorescence after yeast internalisation for each cell.

373 Endocytosis and exocytosis

374 To measure endocytosis, *Dictyostelium* at 5×10^6 cells/ml were shaken at 180 rpm. for 15 mins in
375 HL5 before addition of 100 mg/ml FITC dextran (molecular mass, 70 kDa; Sigma). At each time point
376 500 µl of cell suspension were added to 1 ml ice-cold KK2 on ice. Cells were pelleted at 800 x *g* for 2
377 mins and washed once in KK2. The pellet was lysed in 50 mM Na_2HPO_4 pH 9.3 0.2% Triton X-100 and
378 measured in a fluorimeter. To measure exocytosis, cells were prepared as above and incubated in 2
379 mg/ml FITC-dextran overnight. Cells were pelleted, washed twice in HL5 and resuspended in HL5 at 5

380 × 10^6 cells/ml. 500 µl of cell suspension were taken for each time point and treated as described
381 above.

382 Phagocytosis and phagosomal activity assays

383 Phagocytosis of *E. coli* was monitored by the decrease in turbidity of the bacterial suspension of over
384 time as described [86]. An equal volume of 2 × 10^7 *Dictyostelium* cells was added to a bacterial
385 suspension with an $OD_{600\,nm}$ of 0.8, shaking at 180 rpm, and the decrease in $OD_{600\,nm}$ was recorded
386 over time. Phagocytosis of GFP-expressing *M. smegmatis* and 1 µm YG-carboxylated polystyrene
387 beads (Polysciences Inc.) was previously described [49, 87]. 2 × 10^6 *Dictyostelium*/ml were shaken for
388 2 hours at 150 rpm. Either 1 µm beads (at a ratio of 200:1) or *M. smegmatis* (MOI 100) were added,
389 500 µl aliquots of cells were taken at each time point and fluorescence was measured by flow
390 cytometry [49].

391 Phagosomal pH and proteolytic activity were measured by feeding cells either FITC/TRITC or
392 DQgreen- BSA/Alexa 594-labelled 3 µm silica beads (Kisker Biotech) [49]. Briefly, cells were seeded in
393 a 96 well plate before addition of beads, and fluorescence measured on a plate reader over time. pH
394 values were determined by the ratio of FITC to TRITC fluorescence using a calibration curve, and
395 relative proteolysis was normalised to Alexa594 fluorescence.

396 Bacteria killing assay

397 Killing of GFP-expressing *K. aerogenes* was measured as previously described [52]. Briefly, 10 µl of an
398 overnight culture of bacteria in 280 µl HL5 was placed in a glass-bottomed dish and allowed to settle
399 before careful addition of 1.5 ml of a *Dictyostelium* cell suspension at 1 × 10^6 cells/ml. Images were
400 taken every 20 s for 40 min at 20x magnification. Survival time was determined by how long the GFP-
401 fluorescence persisted after phagocytosis.

402 Western blotting

403 Ax2 or *PIKfyve* null cells expressing GFP-VatM or VatB-GFP were analysed by SDS-PAGE and Western
404 blots using a rabbit anti-GFP primary antibody (gift from A. Peden) and a fluorescently conjugated
405 anti-rabbit 800 secondary antibody, using standard techniques. The endogenous biotinylated
406 mitochondrial protein MCCC1 was used as a loading control using Alexa680-conjugated Streptavadin
407 (Life Technologies) [88].

408 *Legionella* infection assays

409 The following *L. pneumophila* Philadelphia-1 strains were used: virulent JR32 [89], the isogenic Δ*icmT*
410 deletion mutant GS3011 lacking a functional Icm/Dot type 4 secretion system [64], and
411 corresponding strains constitutively producing GFP [65]. *L. pneumophila* was grown for 3 d on

412 charcoal yeast extract (CYE) agar plates, buffered with *N*-(2-acetamido)-2-aminoethane-sulfonic acid
413 (ACES) [90]. For infections, liquid cultures were inoculated in AYE medium at an OD_{600} of 0.1 and
414 grown for 21 h at 37 °C (post-exponential growth phase). To maintain plasmids, chloramphenicol
415 was added at 5 µg/ml.

416 Uptake by *D. discoideum*, intracellular replication or killing of GFP-producing *L. pneumophila* was
417 analyzed by flow cytometry as described [62]. Exponentially growing amoebae were seeded onto a
418 24-well plate (5×10^5 cells/ml HL5 medium per well) and allowed to adhere for 1–2 h. *L.*
419 *pneumophila* grown for 21 h in AYE medium was diluted in HL5 medium and used to infect the
420 amoebae at an MOI of 100 or at the MOI indicated. The infection was synchronized by centrifugation
421 (10 min, 880 *g*), infected cells were incubated at 25 °C and, 30 min post-infection, extracellular
422 bacteria were removed by washing three to five times with SorC (2 mM Na_2HPO_4, 15 mM KH_2PO_4, 50
423 µM $CaCl_2$, pH 6.0). Infected amoebae were detached by vigorously pipetting, and 2×10^4 amoebae
424 per sample were analyzed using a FACSCalibur flow cytometer (Becton Dickinson). The GFP
425 fluorescence intensity falling into a *Dictyostelium* scatter gate was quantified using FlowJo software
426 (Treestar, http://www.treestar.com).

427 Alternatively, intracellular replication of *L. pneumophila* in *D. discoideum* was quantified by
428 determining colony forming units (CFU) in the supernatant as described [62, 91]. Exponentially
429 growing amoebae were washed with SorC and resuspended in MB medium (7 g of yeast extract, 14 g
430 of thiotone E peptone, 20 mM MES in 1 l of H_2O, pH 6.9). Amoebae (1×10^5 cells per well) were
431 seeded onto a 96-well plate, allowed to adhere for 1–2 h, and infected at an MOI of 1 with *L.*
432 *pneumophila* grown in AYE medium for 21 h and diluted in MB medium. The infection was
433 synchronized by centrifugation, and the infected amoebae were incubated at 25 °C. At the time
434 points indicated, the number of bacteria released into the supernatant was quantified by plating
435 aliquots (10–20 µl) of appropriate dilutions on CYE plates. Intracellular bacteria were also quantified
436 by counting CFU after lysis of the infected amoebae with saponin. At the time points indicated, MB
437 medium was replaced by 100 µl of 0.8% saponin and incubated for 15 min. The infected cells were
438 lysed by pipetting, and aliquots were plated.

439

440 Acknowledgments

441 The authors would like to thank Steve Dove for many helpful suggestions and comments, as well as
442 Phill Hawkins for his endeavours to separate *Dictyostelium* PIP_2s.

443 References

444 1. Di Paolo G, De Camilli P. Phosphoinositides in cell regulation and membrane dynamics.
445 Nature. 2006;443(7112):651-7. doi: 10.1038/nature05185. PubMed PMID: 17035995.
446 2. Levin R, Grinstein S, Schlam D. Phosphoinositides in phagocytosis and macropinocytosis.
447 Biochim Biophys Acta. 2015;1851(6):805-23. doi: 10.1016/j.bbalip.2014.09.005. PubMed PMID:
448 25238964.
449 3. Gaullier JM, Simonsen A, D'Arrigo A, Bremnes B, Stenmark H, Aasland R. FYVE fingers bind
450 PtdIns(3)P. Nature. 1998;394(6692):432-3. doi: 10.1038/28767. PubMed PMID: 9697764.
451 4. Raiborg C, Bremnes B, Mehlum A, Gillooly DJ, D'Arrigo A, Stang E, et al. FYVE and coiled-coil
452 domains determine the specific localisation of Hrs to early endosomes. J Cell Sci. 2001;114(Pt
453 12):2255-63. PubMed PMID: 11493665.
454 5. Cabezas A, Pattni K, Stenmark H. Cloning and subcellular localization of a human
455 phosphatidylinositol 3-phosphate 5-kinase, PIKfyve/Fab1. Gene. 2006;371(1):34-41. doi:
456 10.1016/j.gene.2005.11.009. PubMed PMID: 16448788.
457 6. Michell RH, Heath VL, Lemmon MA, Dove SK. Phosphatidylinositol 3,5-bisphosphate:
458 metabolism and cellular functions. Trends Biochem Sci. 2006;31(1):52-63. doi:
459 10.1016/j.tibs.2005.11.013. PubMed PMID: 16364647.
460 7. Sbrissa D, Ikonomov OC, Shisheva A. PIKfyve, a mammalian ortholog of yeast Fab1p lipid
461 kinase, synthesizes 5-phosphoinositides. Effect of insulin. J Biol Chem. 1999;274(31):21589-97.
462 PubMed PMID: 10419465.
463 8. Zolov SN, Bridges D, Zhang Y, Lee WW, Riehle E, Verma R, et al. In vivo, Pikfyve generates
464 PI(3,5)P2, which serves as both a signaling lipid and the major precursor for PI5P. Proc Natl Acad Sci
465 U S A. 2012;109(43):17472-7. doi: 10.1073/pnas.1203106109. PubMed PMID: 23047693; PubMed
466 Central PMCID: PMCPMC3491506.
467 9. Yamamoto A, DeWald DB, Boronenkov IV, Anderson RA, Emr SD, Koshland D. Novel PI(4)P 5-
468 kinase homologue, Fab1p, essential for normal vacuole function and morphology in yeast. Mol Biol
469 Cell. 1995;6(5):525-39. PubMed PMID: 7663021; PubMed Central PMCID: PMCPMC301213.
470 10. Takasuga S, Sasaki T. Phosphatidylinositol-3,5-bisphosphate: metabolism and physiological
471 functions. J Biochem. 2013;154(3):211-8. doi: 10.1093/jb/mvt064. PubMed PMID: 23857703.
472 11. McCartney AJ, Zhang Y, Weisman LS. Phosphatidylinositol 3,5-bisphosphate: low abundance,
473 high significance. BioEssays : news and reviews in molecular, cellular and developmental biology.
474 2014;36(1):52-64. doi: 10.1002/bies.201300012. PubMed PMID: 24323921; PubMed Central PMCID:
475 PMCPMC3906640.
476 12. Ho CY, Alghamdi TA, Botelho RJ. Phosphatidylinositol-3,5-bisphosphate: no longer the poor
477 PIP2. Traffic. 2012;13(1):1-8. doi: 10.1111/j.1600-0854.2011.01246.x. PubMed PMID: 21736686.
478 13. Michell RH. Inositol lipids: from an archaeal origin to phosphatidylinositol 3,5-bisphosphate
479 faults in human disease. FEBS J. 2013;280(24):6281-94. doi: 10.1111/febs.12452. PubMed PMID:
480 23902363.
481 14. Ikonomov O, Sbrissa D, Shisheva A. Mammalian cell morphology and endocytic membrane
482 homeostasis require enzymatically active phosphoinositide 5-kinase PIKfyve. J Biol Chem.
483 2001;276(28):26141-7. doi: 10.1074/jbc.M101722200. PubMed PMID: 11285266.
484 15. Ikonomov OC, Sbrissa D, Mlak K, Deeb R, Fligger J, Soans A, et al. Active PIKfyve associates
485 with and promotes the membrane attachment of the late endosome-to-trans-Golgi network
486 transport factor Rab9 effector p40. J Biol Chem. 2003;278(51):50863-71. doi:
487 10.1074/jbc.M307260200. PubMed PMID: 14530284.
488 16. Rutherford AC, Traer C, Wassmer T, Pattni K, Bujny MV, Carlton JG, et al. The mammalian
489 phosphatidylinositol 3-phosphate 5-kinase (PIKfyve) regulates endosome-to-TGN retrograde
490 transport. J Cell Sci. 2006;119(Pt 19):3944-57. doi: 10.1242/jcs.03153. PubMed PMID: 16954148;
491 PubMed Central PMCID: PMC1904490.

17. de Lartigue J, Polson H, Feldman M, Shokat K, Tooze SA, UrbÃ© S, et al. PIKfyve Regulation of Endosome-Linked Pathways. Traffic. 2009;10(7):883-93. doi: 10.1111/j.1600-0854.2009.00915.x.
18. Martin S, Harper CB, May LM, Coulson EJ, Meunier FA, Osborne SL. Inhibition of PIKfyve by YM-201636 dysregulates autophagy and leads to apoptosis-independent neuronal cell death. PLoS One. 2013;8(3):e60152. doi: 10.1371/journal.pone.0060152. PubMed PMID: 23544129; PubMed Central PMCID: PMC3609765.
19. Rusten T, Vaccari T, Lindmo K, Rodahl L, Nezis I, Sem-Jacobsen C, et al. ESCRTs and Fab1 regulate distinct steps of autophagy. Curr Biol. 2007;17(20):1817-25. doi: 10.1016/j.cub.2007.09.032. PubMed PMID: 17935992.
20. Tsuruta F, Green EM, Rousset M, Dolmetsch RE. PIKfyve regulates CaV1.2 degradation and prevents excitotoxic cell death. J Cell Biol. 2009;187(2):279-94. doi: 10.1083/jcb.200903028. PubMed PMID: 19841139; PubMed Central PMCID: PMC2768838.
21. Min SH, Suzuki A, Stalker TJ, Zhao L, Wang Y, McKennan C, et al. Loss of PIKfyve in platelets causes a lysosomal disease leading to inflammation and thrombosis in mice. Nat Commun. 2014;5:4691. doi: 10.1038/ncomms5691. PubMed PMID: 25178411; PubMed Central PMCID: PMCPMC4369914.
22. Zhang X, Chow CY, Sahenk Z, Shy ME, Meisler MH, Li J. Mutation of FIG4 causes a rapidly progressive, asymmetric neuronal degeneration. Brain : a journal of neurology. 2008;131(Pt 8):1990-2001. doi: 10.1093/brain/awn114. PubMed PMID: 18556664; PubMed Central PMCID: PMC2724900.
23. Zhang Y, McCartney AJ, Zolov SN, Ferguson CJ, Meisler MH, Sutton MA, et al. Modulation of synaptic function by VAC14, a protein that regulates the phosphoinositides PI(3,5)P(2) and PI(5)P. EMBO J. 2012;31(16):3442-56. doi: 10.1038/emboj.2012.200. PubMed PMID: 22842785; PubMed Central PMCID: PMC3419932.
24. Zhang Y, Zolov SN, Chow CY, Slutsky SG, Richardson SC, Piper RC, et al. Loss of Vac14, a regulator of the signaling lipid phosphatidylinositol 3,5-bisphosphate, results in neurodegeneration in mice. Proc Natl Acad Sci U S A. 2007;104(44):17518-23. doi: 10.1073/pnas.0702275104. PubMed PMID: 17956977; PubMed Central PMCID: PMC2077288.
25. Bohdanowicz M, Grinstein S. Role of phospholipids in endocytosis, phagocytosis, and macropinocytosis. Physiological reviews. 2013;93(1):69-106. doi: 10.1152/physrev.00002.2012. PubMed PMID: 23303906.
26. Ellson CD, Anderson KE, Morgan G, Chilvers ER, Lipp P, Stephens LR, et al. Phosphatidylinositol 3-phosphate is generated in phagosomal membranes. Curr Biol. 2001;11(20):1631-5. PubMed PMID: 11676926.
27. Vieira OV, Botelho RJ, Rameh L, Brachmann SM, Matsuo T, Davidson HW, et al. Distinct roles of class I and class III phosphatidylinositol 3-kinases in phagosome formation and maturation. J Cell Biol. 2001;155(1):19-25. doi: 10.1083/jcb.200107069. PubMed PMID: 11581283; PubMed Central PMCID: PMCPMC2150784.
28. Fratti RA, Backer JM, Gruenberg J, Corvera S, Deretic V. Role of phosphatidylinositol 3-kinase and Rab5 effectors in phagosomal biogenesis and mycobacterial phagosome maturation arrest. J Cell Biol. 2001;154(3):631-44. doi: 10.1083/jcb.200106049. PubMed PMID: 11489920; PubMed Central PMCID: PMCPMC2196432.
29. Cai X, Xu Y, Cheung AK, Tomlinson RC, Alcazar-Roman A, Murphy L, et al. PIKfyve, a class III PI kinase, is the target of the small molecular IL-12/IL-23 inhibitor apilimod and a player in Toll-like receptor signaling. Chem Biol. 2013;20(7):912-21. doi: 10.1016/j.chembiol.2013.05.010. PubMed PMID: 23890009.
30. Ikonomov OC, Sbrissa D, Shisheva A. YM201636, an inhibitor of retroviral budding and PIKfyve-catalyzed PtdIns(3,5)P2 synthesis, halts glucose entry by insulin in adipocytes. Biochem Biophys Res Commun. 2009;382(3):566-70. doi: 10.1016/j.bbrc.2009.03.063. PubMed PMID: 19289105; PubMed Central PMCID: PMC3910513.

31. Hazeki K, Nigorikawa K, Takaba Y, Segawa T, Nukuda A, Masuda A, et al. Essential roles of PIKfyve and PTEN on phagosomal phosphatidylinositol 3-phosphate dynamics. FEBS Lett. 2012;586(22):4010-5. doi: 10.1016/j.febslet.2012.09.043. PubMed PMID: 23068606.
32. Kim GH, Dayam RM, Prashar A, Terebiznik M, Botelho RJ. PIKfyve Inhibition Interferes with Phagosome and Endosome Maturation in Macrophages. Traffic. 2014;15(10):1143-63. doi: 10.1111/tra.12199. PubMed PMID: 25041080.
33. Clark J, Kay RR, Kielkowska A, Niewczas I, Fets L, Oxley D, et al. Dictyostelium uses ether-linked inositol phospholipids for intracellular signalling. EMBO J. 2014;33(19):2188-200. doi: 10.15252/embj.201488677. PubMed PMID: 25180230; PubMed Central PMCID: PMCPMC4282506.
34. Calvo-Garrido J, King JS, Munoz-Braceras S, Escalante R. Vmp1 regulates PtdIns3P signaling during autophagosome formation in Dictyostelium discoideum. Traffic. 2014;15(11):1235-46. doi: 10.1111/tra.12210. PubMed PMID: 25131297.
35. King JS, Teo R, Ryves J, Reddy JV, Peters O, Orabi B, et al. The mood stabiliser lithium suppresses PIP3 signalling in Dictyostelium and human cells. Dis Model Mech. 2009;2(5-6):306-12. doi: 10.1242/dmm.001271. PubMed PMID: 19383941; PubMed Central PMCID: PMC2675811.
36. Kortholt A, King JS, Keizer-Gunnink I, Harwood AJ, Van Haastert PJ. Phospholipase C regulation of phosphatidylinositol 3,4,5-trisphosphate-mediated chemotaxis. Mol Biol Cell. 2007;18(12):4772-9. doi: 10.1091/mbc.E07-05-0407. PubMed PMID: 17898079; PubMed Central PMCID: PMC2096598.
37. Dormann D, Weijer G, Dowler S, Weijer CJ. In vivo analysis of 3-phosphoinositide dynamics during Dictyostelium phagocytosis and chemotaxis. J Cell Sci. 2004;117(Pt 26):6497-509. doi: 10.1242/jcs.01579. PubMed PMID: 15572406.
38. Nicot AS, Fares H, Payrastre B, Chisholm AD, Labouesse M, Laporte J. The phosphoinositide kinase PIKfyve/Fab1p regulates terminal lysosome maturation in Caenorhabditis elegans. Molecular biology of the cell. 2006;17(7):3062-74. PubMed PMID: WOS:000238721000018.
39. Smith EW, Lima WC, Charette SJ, Cosson P. Effect of starvation on the endocytic pathway in Dictyostelium cells. Eukaryot Cell. 2010;9(3):387-92. doi: 10.1128/EC.00285-09. PubMed PMID: 20097741; PubMed Central PMCID: PMCPMC2837978.
40. Veltman DM, Williams TD, Bloomfield G, Chen BC, Betzig E, Insall RH, et al. A plasma membrane template for macropinocytic cups. eLife. 2016;5. doi: 10.7554/eLife.20085. PubMed PMID: 27960076; PubMed Central PMCID: PMCPMC5154761.
41. Clarke M, Maddera L, Engel U, Gerisch G. Retrieval of the vacuolar H-ATPase from phagosomes revealed by live cell imaging. PLoS One. 2010;5(1):e8585. doi: 10.1371/journal.pone.0008585. PubMed PMID: 20052281; PubMed Central PMCID: PMCPMC2796722.
42. Simonsen A, Lippe R, Christoforidis S, Gaullier JM, Brech A, Callaghan J, et al. EEA1 links PI(3)K function to Rab5 regulation of endosome fusion. Nature. 1998;394(6692):494-8. doi: 10.1038/28879. PubMed PMID: 9697774.
43. Gillooly DJ, Morrow IC, Lindsay M, Gould R, Bryant NJ, Gaullier JM, et al. Localization of phosphatidylinositol 3-phosphate in yeast and mammalian cells. Embo Journal. 2000;19(17):4577-88. doi: 10.1093/emboj/19.17.4577. PubMed PMID: WOS:000089275600016.
44. Clarke M, Kohler J, Arana Q, Liu T, Heuser J, Gerisch G. Dynamics of the vacuolar H(+)-ATPase in the contractile vacuole complex and the endosomal pathway of Dictyostelium cells. J Cell Sci. 2002;115(Pt 14):2893-905. PubMed PMID: 12082150.
45. Gary JD, Wurmser AE, Bonangelino CJ, Weisman LS, Emr SD. Fab1p is essential for PtdIns(3)P 5-kinase activity and the maintenance of vacuolar size and membrane homeostasis. J Cell Biol. 1998;143(1):65-79. PubMed PMID: 9763421; PubMed Central PMCID: PMC2132800.
46. Jefferies HB, Cooke FT, Jat P, Boucheron C, Koizumi T, Hayakawa M, et al. A selective PIKfyve inhibitor blocks PtdIns(3,5)P(2) production and disrupts endomembrane transport and retroviral budding. EMBO reports. 2008;9(2):164-70. doi: 10.1038/sj.embor.7401155. PubMed PMID: 18188180; PubMed Central PMCID: PMCPMC2246419.

592 47. Kerr MC, Wang JT, Castro NA, Hamilton NA, Town L, Brown DL, et al. Inhibition of the PtdIns
593 (5) kinase PIKfyve disrupts intracellular replication of Salmonella. The EMBO journal.
594 2010;29(8):1331-47.
595 48. Bak G, Lee EJ, Lee Y, Kato M, Segami S, Sze H, et al. Rapid structural changes and acidification
596 of guard cell vacuoles during stomatal closure require phosphatidylinositol 3,5-bisphosphate. Plant
597 Cell. 2013;25(6):2202-16. doi: 10.1105/tpc.113.110411. PubMed PMID: 23757398; PubMed Central
598 PMCID: PMC3723621.
599 49. Sattler N, Monroy R, Soldati T. Quantitative analysis of phagocytosis and phagosome
600 maturation. Methods in molecular biology. 2013;983:383-402. doi: 10.1007/978-1-62703-302-2_21.
601 PubMed PMID: 23494319.
602 50. Li SC, Diakov TT, Xu T, Tarsio M, Zhu W, Couoh-Cardel S, et al. The signaling lipid PI(3,5)P(2)
603 stabilizes V(1)-V(o) sector interactions and activates the V-ATPase. Mol Biol Cell. 2014;25(8):1251-62.
604 doi: 10.1091/mbc.E13-10-0563. PubMed PMID: 24523285; PubMed Central PMCID:
605 PMCPMC3982991.
606 51. Park L, Thomason PA, Zech T, King JS, Veltman DM, Carnell M, et al. Cyclical action of the
607 WASH complex: FAM21 and capping protein drive WASH recycling, not initial recruitment. Dev Cell.
608 2013;24(2):169-81. doi: 10.1016/j.devcel.2012.12.014. PubMed PMID: 23369714.
609 52. Leiba J, Sabra A, Bodinier R, Marchetti A, Lima WC, Melotti A, et al. Vps13F links bacterial
610 recognition and intracellular killing in Dictyostelium. Cell Microbiol. 2017. doi: 10.1111/cmi.12722.
611 PubMed PMID: 28076662.
612 53. Hilbi H, Hoffmann C, Harrison CF. Legionella spp. outdoors: colonization, communication and
613 persistence. Environ Microbiol Rep. 2011;3(3):286-96. doi: 10.1111/j.1758-2229.2011.00247.x.
614 PubMed PMID: 23761274.
615 54. Finsel I, Hilbi H. Formation of a pathogen vacuole according to Legionella pneumophila: how
616 to kill one bird with many stones. Cell Microbiol. 2015;17(7):935-50. doi: 10.1111/cmi.12450.
617 PubMed PMID: 25903720.
618 55. Ge J, Shao F. Manipulation of host vesicular trafficking and innate immune defence by
619 Legionella Dot/Icm effectors. Cell Microbiol. 2011;13(12):1870-80. doi: 10.1111/j.1462-
620 5822.2011.01710.x. PubMed PMID: 21981078.
621 56. Weber S, Wagner M, Hilbi H. Live-cell imaging of phosphoinositide dynamics and membrane
622 architecture during Legionella infection. MBio. 2014;5(1):e00839-13. doi: 10.1128/mBio.00839-13.
623 PubMed PMID: 24473127; PubMed Central PMCID: PMCPMC3903275.
624 57. Brombacher E, Urwyler S, Ragaz C, Weber SS, Kami K, Overduin M, et al. Rab1 guanine
625 nucleotide exchange factor SidM is a major phosphatidylinositol 4-phosphate-binding effector
626 protein of Legionella pneumophila. J Biol Chem. 2009;284(8):4846-56. doi:
627 10.1074/jbc.M807505200. PubMed PMID: 19095644; PubMed Central PMCID: PMC2643517.
628 58. Hilbi H, Weber S, Finsel I. Anchors for effectors: subversion of phosphoinositide lipids by
629 legionella. Front Microbiol. 2011;2:91. doi: 10.3389/fmicb.2011.00091. PubMed PMID: 21833330;
630 PubMed Central PMCID: PMC3153050.
631 59. Jank T, Bohmer KE, Tzivelekidis T, Schwan C, Belyi Y, Aktories K. Domain organization of
632 Legionella effector SetA. Cell Microbiol. 2012;14(6):852-68. doi: 10.1111/j.1462-5822.2012.01761.x.
633 PubMed PMID: 22288428.
634 60. Finsel I, Ragaz C, Hoffmann C, Harrison CF, Weber S, van Rahden VA, et al. The Legionella
635 effector RidL inhibits retrograde trafficking to promote intracellular replication. Cell Host Microbe.
636 2013;14(1):38-50. doi: 10.1016/j.chom.2013.06.001. PubMed PMID: 23870312.
637 61. Harding CR, Mattheis C, Mousnier A, Oates CV, Hartland EL, Frankel G, et al. LtpD Is a Novel
638 Legionella pneumophila Effector That Binds Phosphatidylinositol 3-Phosphate and Inositol
639 Monophosphatase IMPA1. Infection and Immunity. 2013;81(11):4261-70. doi: 10.1128/iai.01054-13.
640 PubMed PMID: WOS:000325719900031.

641 62. Weber SS, Ragaz C, Reus K, Nyfeler Y, Hilbi H. Legionella pneumophila exploits PI(4)P to
642 anchor secreted effector proteins to the replicative vacuole. Plos Pathogens. 2006;2(5):418-30. doi:
643 ARTN e46

644 10.1371/journal.ppat.0020046. PubMed PMID: WOS:000202894500009.
645 63. Dolinsky S, Haneburger I, Cichy A, Hannemann M, Itzen A, Hilbi H. The Legionella
646 longbeachae Icm/Dot substrate SidC selectively binds phosphatidylinositol 4-phosphate with
647 nanomolar affinity and promotes pathogen vacuole-endoplasmic reticulum interactions. Infect
648 Immun. 2014;82(10):4021-33. doi: 10.1128/IAI.01685-14. PubMed PMID: 25024371; PubMed
649 Central PMCID: PMCPMC4187854.
650 64. Segal G, Shuman HA. Intracellular multiplication and human macrophage killing by Legionella
651 pneumophila are inhibited by conjugal components of IncQ plasmid RSF1010. Molecular
652 Microbiology. 1998;30(1):197-208. doi: 10.1046/j.1365-2958.1998.01054.x. PubMed PMID:
653 WOS:000076538500017.
654 65. Hilbi H, Segal G, Shuman HA. Icm/dot-dependent upregulation of phagocytosis by Legionella
655 pneumophila. Mol Microbiol. 2001;42(3):603-17. PubMed PMID: 11722729.
656 66. Rizopoulos Z, Balistreri G, Kilcher S, Martin CK, Syedbasha M, Helenius A, et al. Vaccinia Virus
657 Infection Requires Maturation of Macropinosomes. Traffic. 2015;16(8):814-31. doi:
658 10.1111/tra.12290. PubMed PMID: 25869659; PubMed Central PMCID: PMCPMC4973667.
659 67. Krishna S, Palm W, Lee Y, Yang W, Bandyopadhyay U, Xu H, et al. PIKfyve Regulates Vacuole
660 Maturation and Nutrient Recovery following Engulfment. Dev Cell. 2016;38(5):536-47. doi:
661 10.1016/j.devcel.2016.08.001. PubMed PMID: 27623384; PubMed Central PMCID:
662 PMCPMC5046836.
663 68. Ho CY, Choy CH, Wattson CA, Johnson DE, Botelho RJ. The Fab1/PIKfyve Phosphoinositide
664 Phosphate Kinase Is Not Necessary to Maintain the pH of Lysosomes and of the Yeast Vacuole. J Biol
665 Chem. 2015;290(15):9919-28. doi: 10.1074/jbc.M114.613984. PubMed PMID: 25713145.
666 69. Dong XP, Shen D, Wang X, Dawson T, Li X, Zhang Q, et al. PI(3,5)P(2) controls membrane
667 trafficking by direct activation of mucolipin Ca(2+) release channels in the endolysosome. Nat
668 Commun. 2010;1:38. doi: 10.1038/ncomms1037. PubMed PMID: 20802798; PubMed Central PMCID:
669 PMCPMC2928581.
670 70. Dayam RM, Saric A, Shilliday RE, Botelho RJ. The Phosphoinositide-Gated Lysosomal Ca(2+)
671 Channel, TRPML1, Is Required for Phagosome Maturation. Traffic. 2015;16(9):1010-26. doi:
672 10.1111/tra.12303. PubMed PMID: 26010303.
673 71. Li X, Rydzewski N, Hider A, Zhang X, Yang J, Wang W, et al. A molecular mechanism to
674 regulate lysosome motility for lysosome positioning and tubulation. Nat Cell Biol. 2016;18(4):404-17.
675 doi: 10.1038/ncb3324. PubMed PMID: 26950892.
676 72. Lima WC, Leuba F, Soldati T, Cosson P. Mucolipin controls lysosome exocytosis in
677 Dictyostelium. J Cell Sci. 2012;125(Pt 9):2315-22. doi: 10.1242/jcs.100362. PubMed PMID: 22357942.
678 73. Horwitz MA. THE LEGIONNAIRES-DISEASE BACTERIUM (LEGIONELLA-PNEUMOPHILA)
679 INHIBITS PHAGOSOME-LYSOSOME FUSION IN HUMAN-MONOCYTES. Journal of Experimental
680 Medicine. 1983;158(6):2108-26. doi: 10.1084/jem.158.6.2108. PubMed PMID:
681 WOS:A1983RV00200023.
682 74. Lamothe J, Huynh KK, Grinstein S, Valvano MA. Intracellular survival of Burkholderia
683 cenocepacia in macrophages is associated with a delay in the maturation of bacteria-containing
684 vacuoles. Cell Microbiol. 2007;9(1):40-53. doi: 10.1111/j.1462-5822.2006.00766.x. PubMed PMID:
685 16869828.
686 75. Smith LM, Dixon EF, May RC. The fungal pathogen Cryptococcus neoformans manipulates
687 macrophage phagosome maturation. Cell Microbiol. 2015;17(5):702-13. doi: 10.1111/cmi.12394.
688 PubMed PMID: 25394938.
689 76. Segal G, Shuman HA. Legionella pneumophila utilizes the same genes to multiply within
690 Acanthamoeba castellanii and human macrophages. Infection and Immunity. 1999;67(5):2117-24.
691 PubMed PMID: WOS:000079909300010.

692 77. Steenbergen JN, Shuman HA, Casadevall A. Cryptococcus neoformans interactions with
693 amoebae suggest an explanation for its virulence and intracellular pathogenic strategy in
694 macrophages. Proc Natl Acad Sci U S A. 2001;98(26):15245-50. doi: 10.1073/pnas.261418798.
695 PubMed PMID: 11742090; PubMed Central PMCID: PMC65014.
696 78. Hasselbring BM, Patel MK, Schell MA. Dictyostelium discoideum as a model system for
697 identification of Burkholderia pseudomallei virulence factors. Infect Immun. 2011;79(5):2079-88.
698 doi: 10.1128/IAI.01233-10. PubMed PMID: 21402765; PubMed Central PMCID: PMC3088138.
699 79. Hubber A, Roy CR. Modulation of host cell function by Legionella pneumophila type IV
700 effectors. Annu Rev Cell Dev Biol. 2010;26:261-83. doi: 10.1146/annurev-cellbio-100109-104034.
701 PubMed PMID: 20929312.
702 80. Isberg RR, O'Connor TJ, Heidtman M. The Legionella pneumophila replication vacuole:
703 making a cosy niche inside host cells. Nature Reviews Microbiology. 2009;7(1):12-24. doi:
704 10.1038/nrmicro1967. PubMed PMID: WOS:000262110300009.
705 81. Froquet R, Lelong E, Marchetti A, Cosson P. Dictyostelium discoideum: a model host to
706 measure bacterial virulence. Nature Protocols. 2009;4(1):25-30. doi: 10.1038/nprot.2008.212.
707 PubMed PMID: WOS:000265781800003.
708 82. Wilkins A, Khosla M, Fraser DJ, Spiegelman GB, Fisher PR, Weeks G, et al. Dictyostelium RasD
709 is required for normal phototaxis, but not differentiation. Genes Dev. 2000;14(11):1407-13. PubMed
710 PMID: 10837033; PubMed Central PMCID: PMCPMC316659.
711 83. Sutoh K. A transformation vector for dictyostelium discoideum with a new selectable marker
712 bsr. Plasmid. 1993;30(2):150-4. doi: 10.1006/plas.1993.1042. PubMed PMID: 8234487.
713 84. Veltman DM, Lemieux MG, Knecht DA, Insall RH. PIP(3)-dependent macropinocytosis is
714 incompatible with chemotaxis. J Cell Biol. 2014;204(4):497-505. doi: 10.1083/jcb.201309081.
715 PubMed PMID: 24535823; PubMed Central PMCID: PMCPMC3926956.
716 85. Carnell M, Zech T, Calaminus SD, Ura S, Hagedorn M, Johnston SA, et al. Actin polymerization
717 driven by WASH causes V-ATPase retrieval and vesicle neutralization before exocytosis. J Cell Biol.
718 2011;193(5):831-9. doi: 10.1083/jcb.201009119. PubMed PMID: 21606208; PubMed Central PMCID:
719 PMC3105540.
720 86. King J, Insall RH. Parasexual genetics of Dictyostelium gene disruptions: identification of a ras
721 pathway using diploids. Bmc Genetics. 2003;4. doi: 10.1186/1471-2156-4-12. PubMed PMID:
722 WOS:000184659500001.
723 87. Arafah S, Kicka S, Trofimov V, Hagedorn M, Andreu N, Wiles S, et al. Setting up and
724 monitoring an infection of Dictyostelium discoideum with mycobacteria. Methods Mol Biol.
725 2013;983:403-17. doi: 10.1007/978-1-62703-302-2_22. PubMed PMID: 23494320.
726 88. Davidson AJ, King JS, Insall RH. The use of streptavidin conjugates as immunoblot loading
727 controls and mitochondrial markers for use with Dictyostelium discoideum. Biotechniques.
728 2013;55(1):39-41. doi: 10.2144/000114054. PubMed PMID: 23834384.
729 89. Sadosky AB, Wiater LA, Shuman HA. Identification of Legionella pneumophila genes required
730 for growth within and killing of human macrophages. Infect Immun. 1993;61(12):5361-73. PubMed
731 PMID: 8225610; PubMed Central PMCID: PMCPMC281323.
732 90. Feeley JC, Gibson RJ, Gorman GW, Langford NC, Rasheed JK, Mackel DC, et al. Charcoal-yeast
733 extract agar: primary isolation medium for Legionella pneumophila. J Clin Microbiol. 1979;10(4):437-
734 41. PubMed PMID: 393713; PubMed Central PMCID: PMCPMC273193.
735 91. Solomon JM, Rupper A, Cardelli JA, Isberg RR. Intracellular growth of Legionella pneumophila
736 in Dictyostelium discoideum, a system for genetic analysis of host-pathogen interactions. Infect
737 Immun. 2000;68(5):2939-47. PubMed PMID: 10768992; PubMed Central PMCID: PMCPMC97507.

738

739

740 ## Figure Legends

741 ### Figure 1

742 **Knockout or inhibition of PIKfyve leads to a swollen vesicle phenotype.** (A) DIC images of Ax3, two
743 independent *PIKfyve*-null clones and a random integrant in HL5 medium. Arrows indicate the
744 enlarged vesicles. (B) Swollen vesicles in *PIKfyve*-null cells became more apparent after incubation
745 for the time indicated in the low osmolarity starvation buffer (KK2), but were lost as cells entered
746 differentiation. (C) Induction of swollen vesicles with 5 µM apilimod, a PIKfyve-specific inhibitor.
747 Images taken in HL5 medium after 5 hours of treatment.

748 ### Figure 2

749 ***PIKfyve* null cells have growth defects**. *PIKfyve*⁻null cells had no defects in either (A) endocytosis or
750 (B) exocytosis, as measured by uptake or loss of FITC dextran. Data shown are mean +/- SD. (C)
751 Despite normal uptake, *PIKfyve*-null cells had a longer generation time than Ax3 cells when growing
752 axenically in liquid culture, data shown are mean +/- SD. (D) *PIKfyve*-null cells grew markedly more
753 slowly on lawns of *Klebsiella pneumophila* than either Ax3 or a random integrant. (E) Growth on
754 bacteria is also defective for *PIKfyve*-null cells in the Ax2 genetic background and across multiple
755 bacterial strains. Growth was assessed by plating serial dilutions of amoebae on lawns of different
756 bacteria and dark patches indicate amoebae growth. Data for all bacteria are summarised in (F).

757 ### Figure 3

758 **Phagocytic uptake is not dependent on PIKfyve.** (A) There was no defect in the ability of *PIKfyve*-null
759 cells to reduce the turbidity of a suspension of *E. coli* over time. (B) Uptake of 1 µm beads or (C) GFP-
760 expressing *Mycobacterium smegmatis* was also not affected by absence of PIKfyve, as measured by
761 flow cytometry. Data shown are means +/- SD.

762 ### Figure 4

763 **PIKfyve is important for acidification and proteolysis.** (A) PI(3)P dynamics are not altered by
764 absence of PIKfyve. PI(3)P was monitored by visualising the recruitment of a GFP-2xFYVE probe to
765 phagosomes following uptake of 3 µm beads (asterisks) by confocal time-lapse microscopy. (B) Time
766 that GFP-2xFYVE stays associated with phagosomes following engulfment, indicating that PI(3)P
767 removal is not PIKfyve-dependent. n indicates the total number of cells quantified in 3 independent
768 experiments. (C) Phagosomal acidification and (D) proteolysis are severely disrupted in *PIKfyve* null
769 cells, measured using 3 µm beads coupled to acidification or proteolysis reporters. Data shown are
770 mean +/- SD.

771 Figure 5

772 **PIKfyve is required for efficient V-ATPase recruitment.** Recruitment of (A) the V-ATPase V_0 subunit
773 GFP-VatM and (B) the V_1 peripheral subunit VatB-GFP to phagocytosed pHrodo-labelled yeast
774 visualised by confocal time-lapse imaging. (C) Quantification of GFP-VatM recruitment over time,
775 indicating reduced recruitment in *PIKfyve*-null mutants. (D) Quantification of VatB-GFP recruitment,
776 following the same pattern. (E) Quantification of increase in yeast-associated pHrodo fluorescence,
777 indicating acidification. The fluorescence increases significantly more in Ax2 cells than in *PIKfyve*-null
778 cells. Data shown are mean +/- SEM, p values calculated by Student's t-test.

779 Figure 6

780 **Bacterial survival is increased in *PIKfyve* null cells.** (A) Kaplan-Meyer survival graph, with survival
781 indicated by persistent fluorescence of phagocytosed GFP-expressing *Klebsiella pneumophila*.
782 Bacteria survived for significantly longer in *PIKfyve*-null cells than in Ax2 ($p<0.0001$ as determined by
783 Mantel-Cox test). 60 bacteria were followed across three independent experiments. (B) Stills from
784 the widefield time-lapse movies quantified in (A). Arrows indicate phagocytosed bacteria

785 Figure 7

786 **PIKfyve is required to suppress *Legionella* replication.** (A) Uptake of GFP-producing wild-type (JR32)
787 or avirulent (Δ*icmT*) *L. pneumophila* by *Dictyostelium* cells (MOI 100), analyzed by flow cytometry.
788 Wild-type *L. pneumophila* show a higher infectivity than the avirulent strain both in Ax3 and in
789 *PIKfyve*$^-$ *Dictyostelium*. (B) Intracellular growth and/or killing of *L. pneumophila* analyzed by colony
790 forming units (CFU): *Dictyostelium* was infected with *L. pneumophila* wild-type (at an MOI of 1) or
791 Δ*icmT* (MOI 100). In the course of multiple infection rounds (release and re-infection), more wild-
792 type *L. pneumophila* accumulated in the medium surrounding *PIKfyve*$^-$ cells than wild-type. in
793 contrast, Δ*icmT* mutant bacteria were killed by both *Dictyostelium* strains. (C) *Dictyostelium* were
794 infected with *L. pneumophila* wild-type (MOI 1) or Δ*icmT* (MOI 100), lysed and intracellular CFU
795 determined. Wild-type *L. pneumophila* grew significantly better in *PIKfyve*$^-$ cells than Ax3. (D)
796 Analysis of intracellular growth of GFP-expressing *L. pneumophila* wild-type JR32 (MOI 1) or Δ*icmT*
797 (MOI 100) by flow cytometry. Virulent *L. pneumophila* replicate more efficiently in *PIKfyve*$^-$
798 *Dictyostelium*, as indicated by the increasing proportions of amoebae containing high levels of GFP
799 over time. Data represent means and standard deviation of duplicates (A; 10,000 counts each; n.s.,
800 not significant) or triplicates (B, C; **, $P < 0.01$) and are representative of 2-3 independent
801 experiments.

802 ## Supplementary Figure 1

803 ***PIKfyve* gene disruption.** (A) Schematic representation of *Dictyostelium* PIKfyve indicating the site
804 where the blasticidin resistance cassette was inserted into the gene to generate knockouts.

805 ## Supplementary Figure 2

806 **PIKfyve is not required for development.** *PIKfyve*$^{-}$ cells formed (A) morphologically normal fruiting
807 bodies as well as (B) normal spores.

808 ## Supplementary Figure 3

809 **VatM expression has a dominant negative effect on acidification.** (A) VatB-GFP expression in Ax2
810 and *PIKfyve*$^{-}$ cells suppressed acidification as measured by increase in pHrodo fluorescence,
811 compared to the increase in fluorescence in cells expressing GFP-VatM. (B) Western blot of cells
812 expressing VatB-GFP or GFP-VatM. There was no difference in expression levels between Ax2 and
813 *PIKfyve*$^{-}$ cells for either reporter. However, VatB-GFP was expressed at a much higher level than GFP-
814 VatM. Loading control is the mitochondrial protein MCCC1, recognised by Alexa680-conjugated
815 streptavidin.

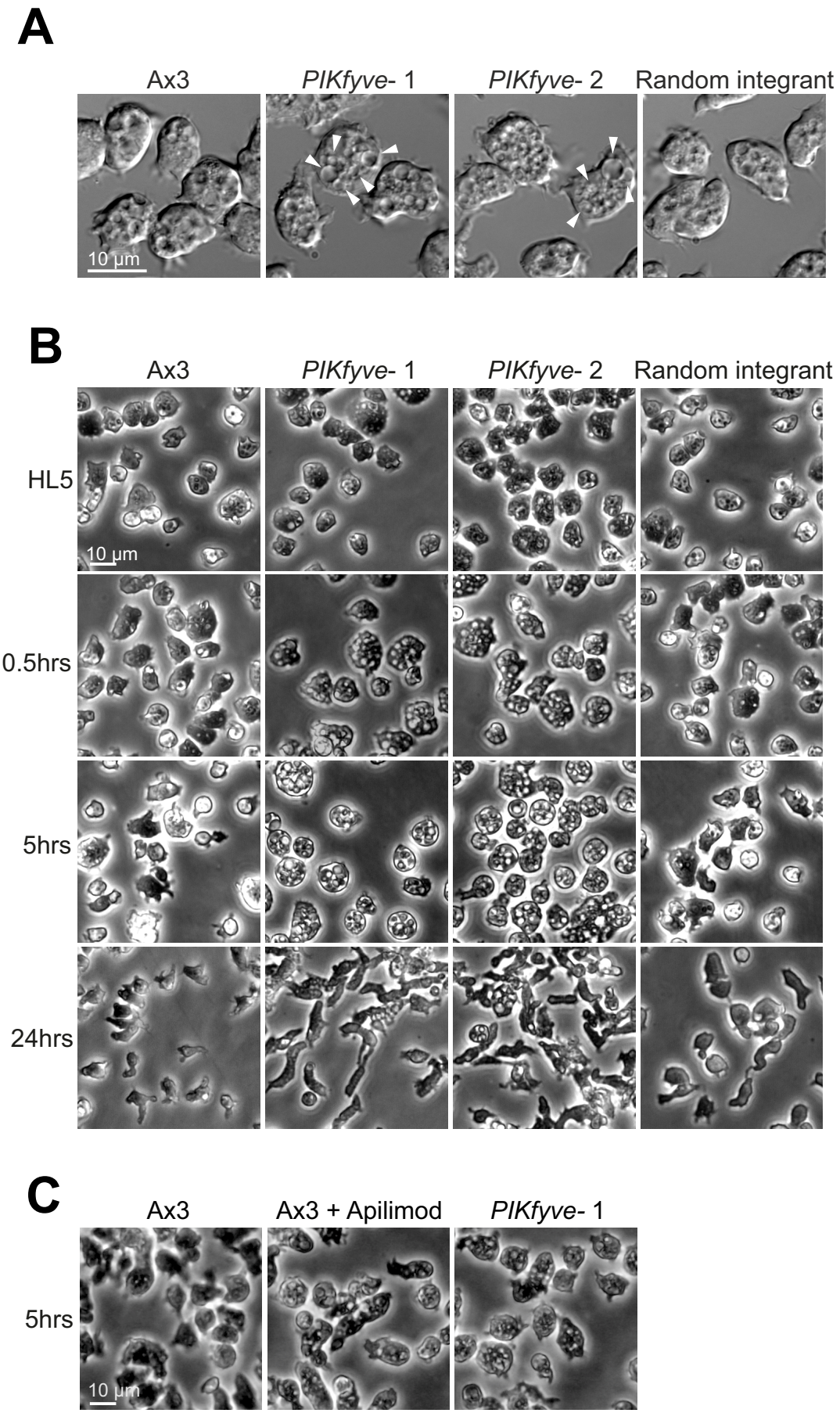

Figure 1: KO or inhibition of PIKfyve leads to a swollen vesicle phenotype

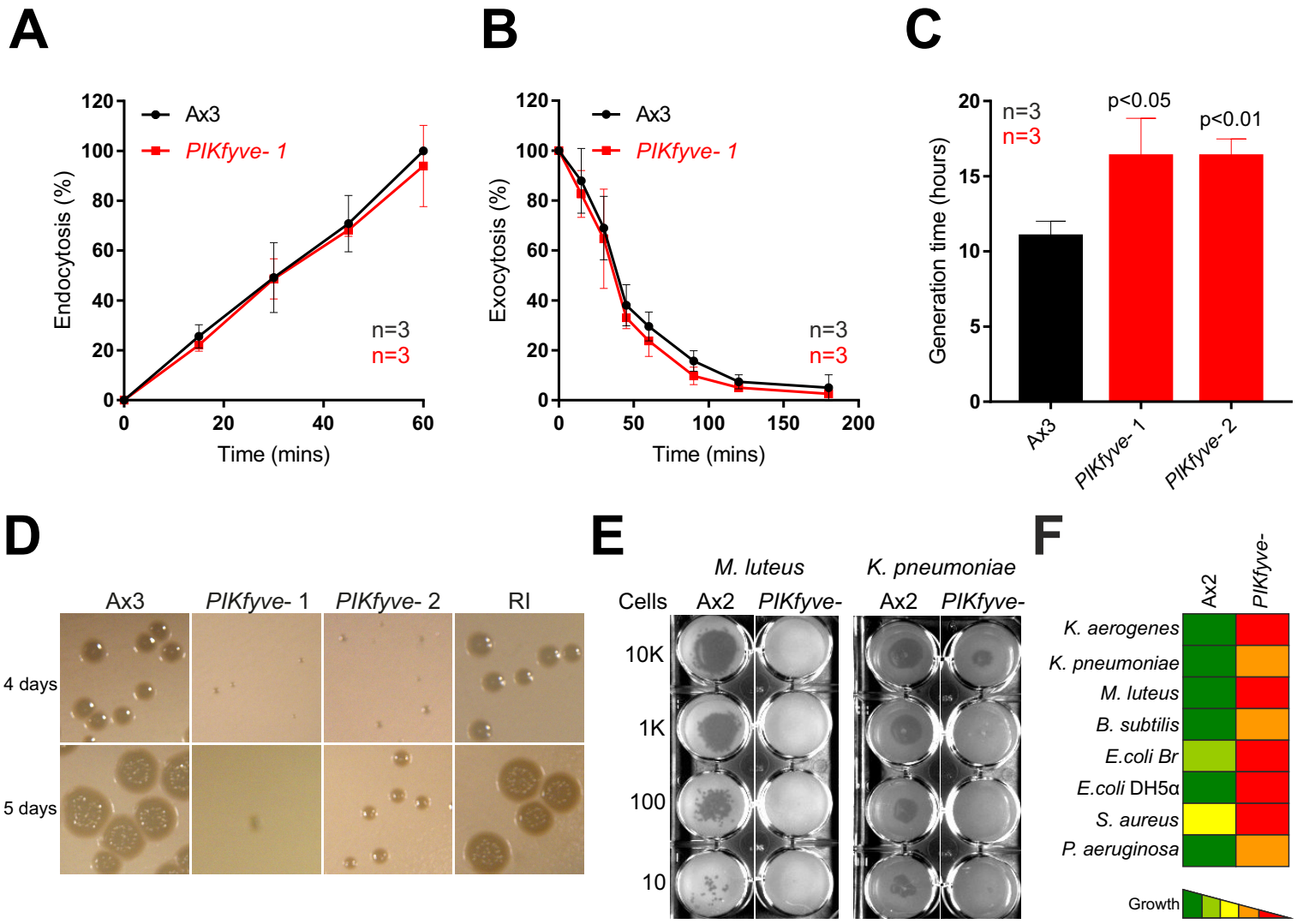

Figure 2: *PIKfyve-* cells have growth defects

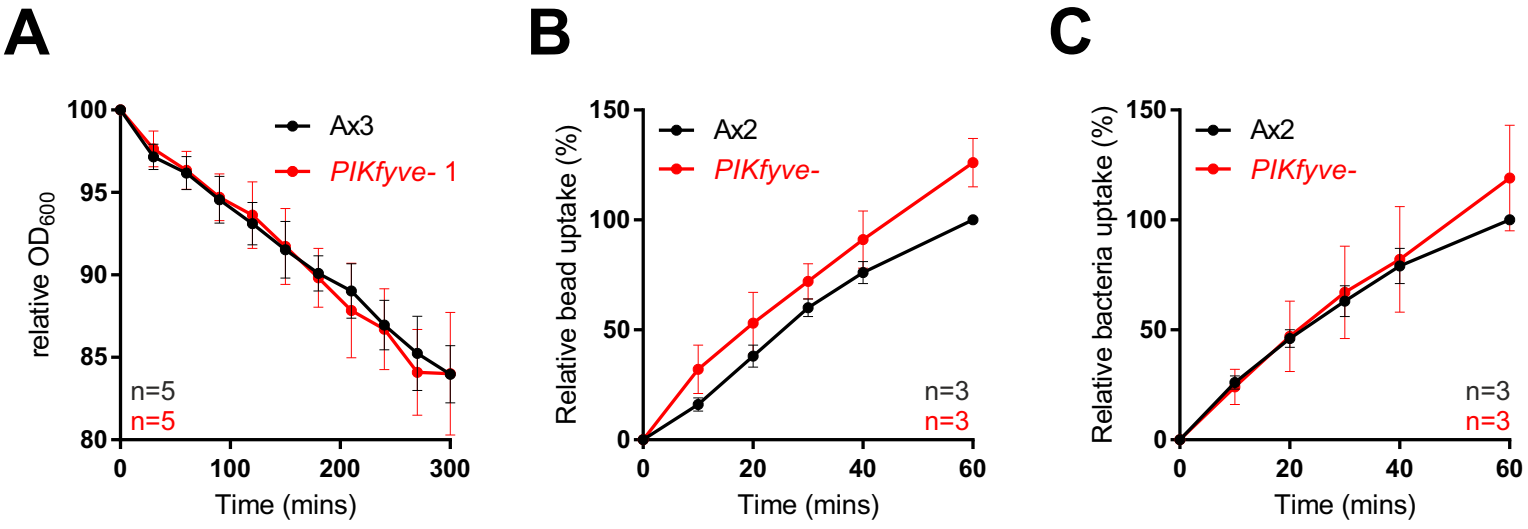

Figure 3: PIKfyve is not required for phagocytic uptake

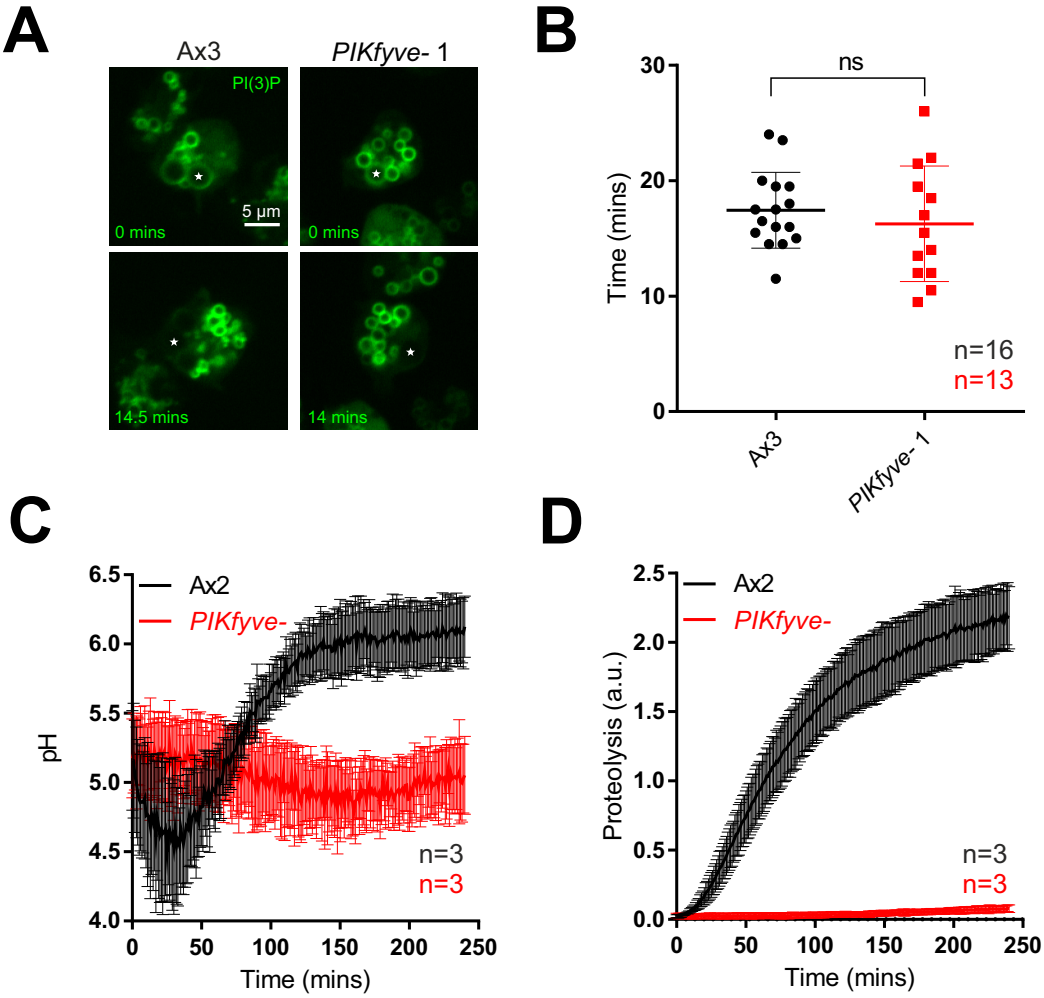

Figure 4: PIKfyve is important for phagosome acidification and proteolysis

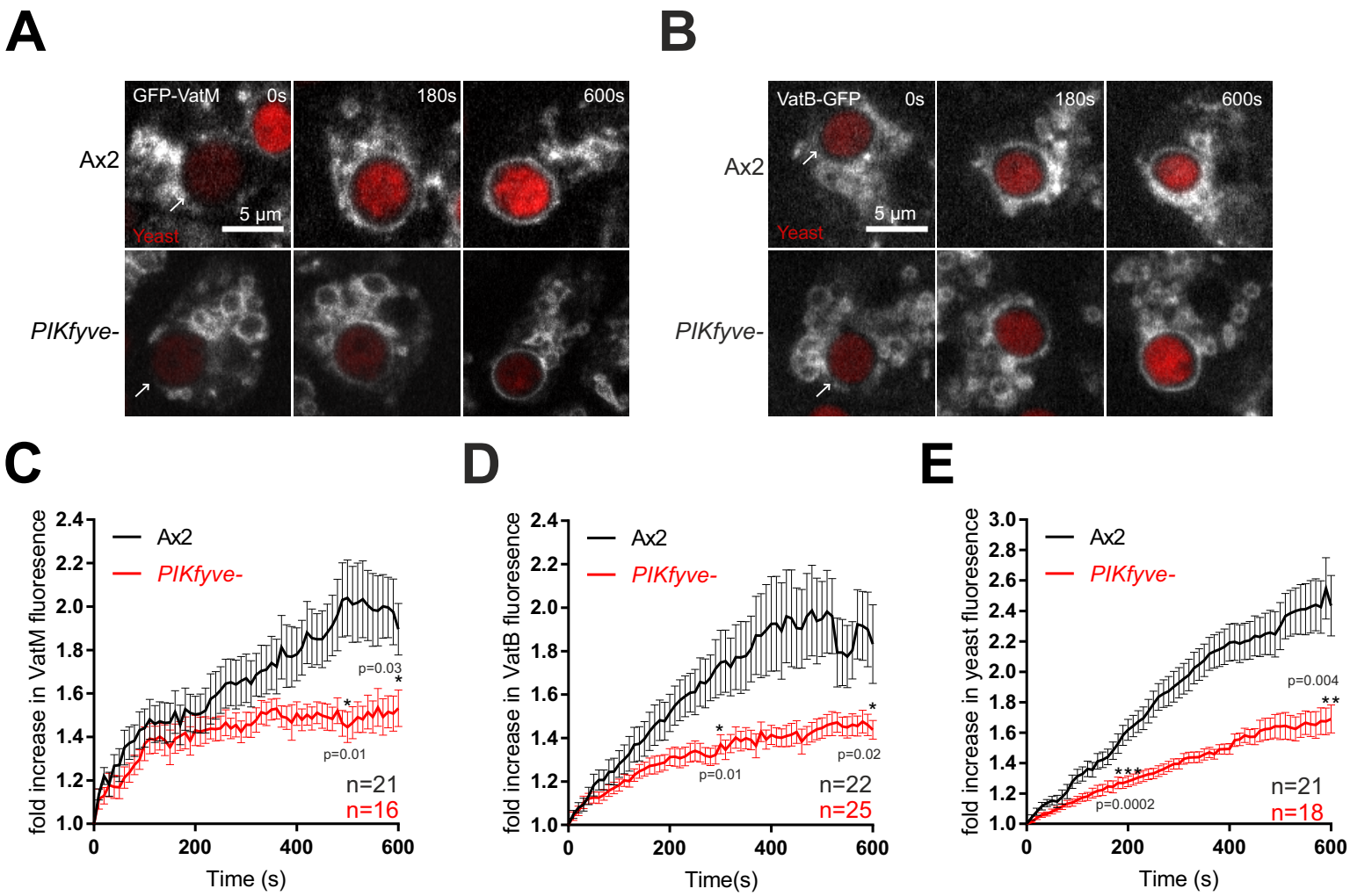

Figure 5: PIKfyve is required for efficient V-ATPase recruitment

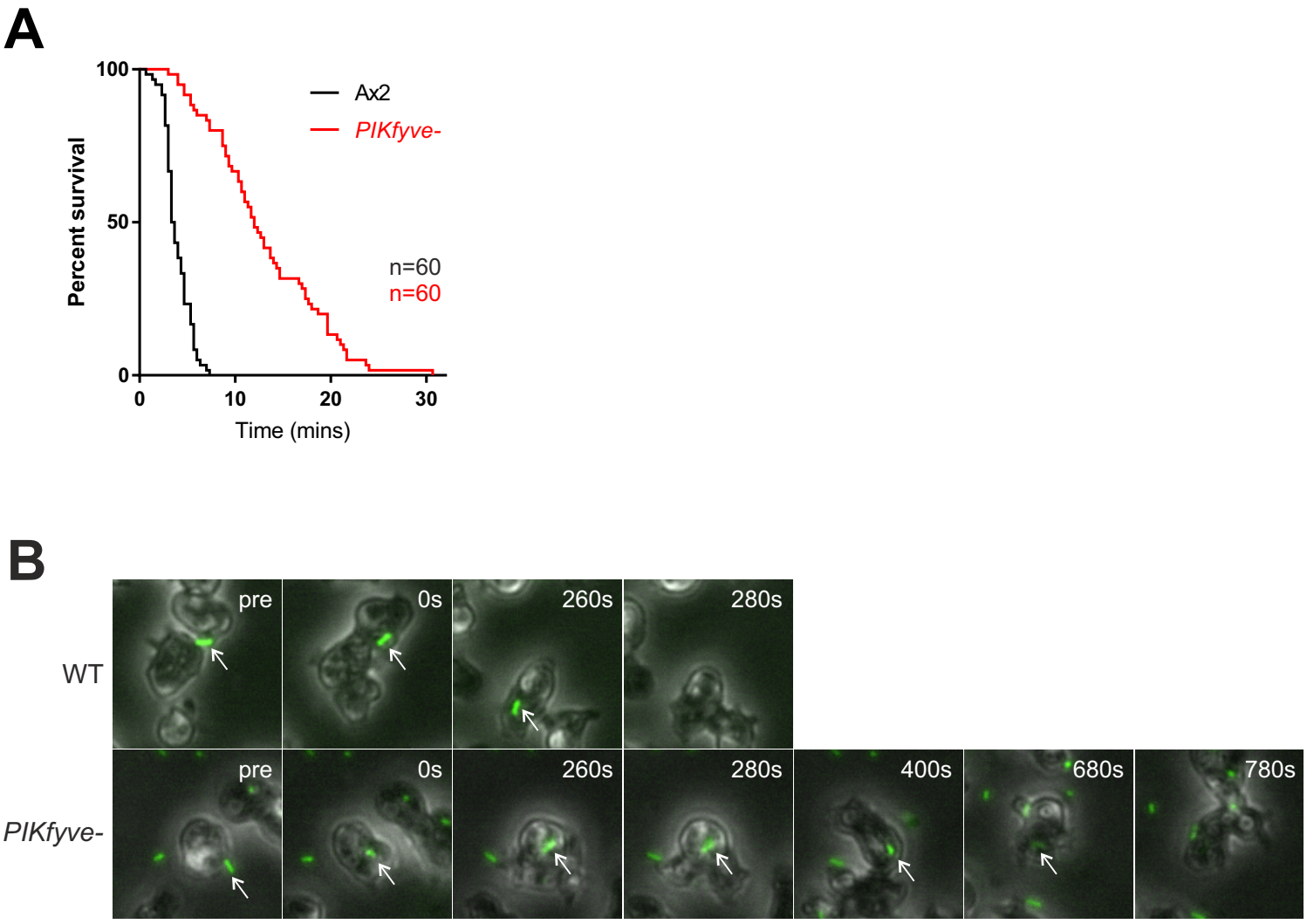

Figure 6: Bacterial survival is increased in *PIKfyve-* cells

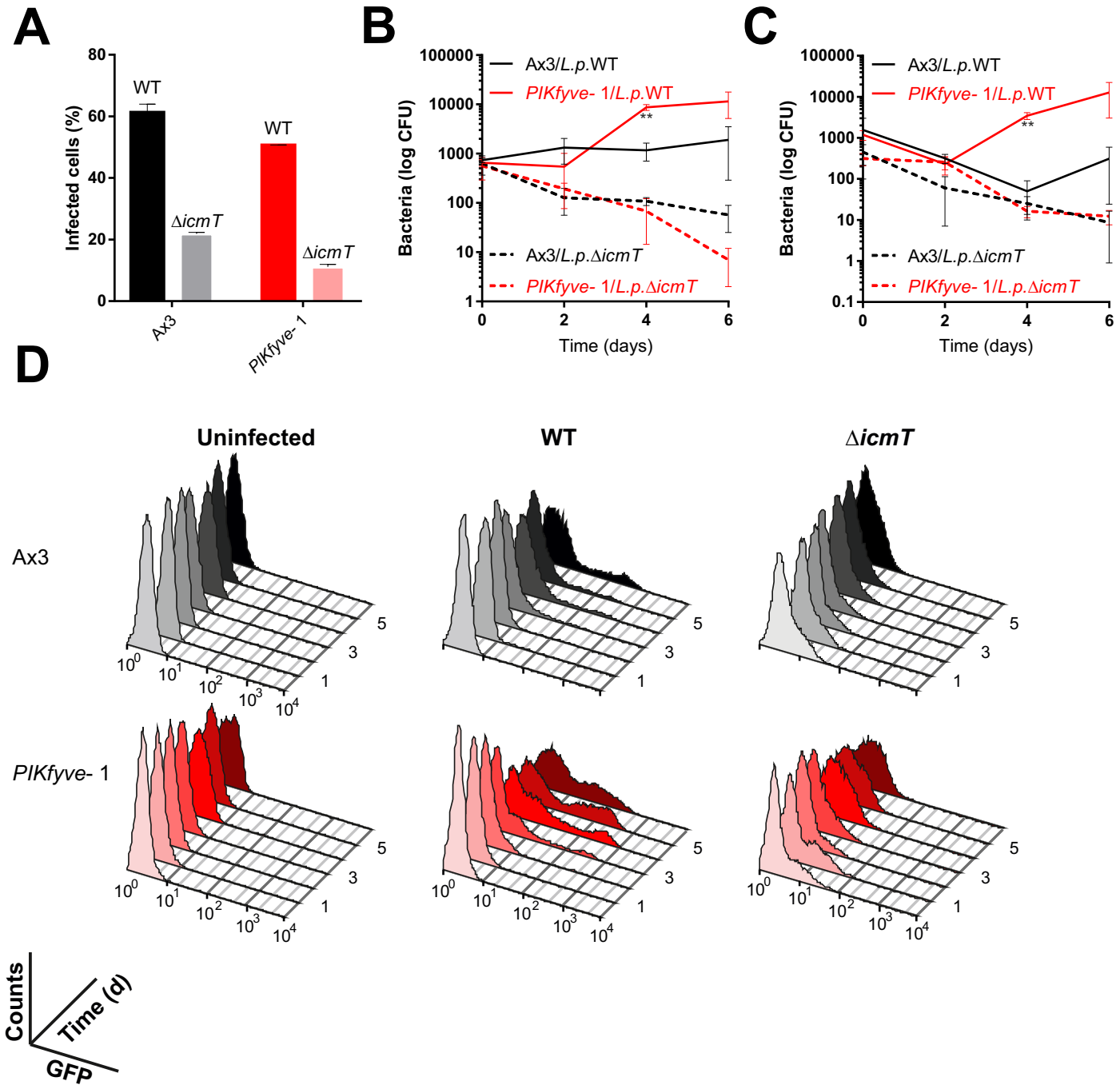

Figure 7: PIKfyve is required to suppress legionella replication

A

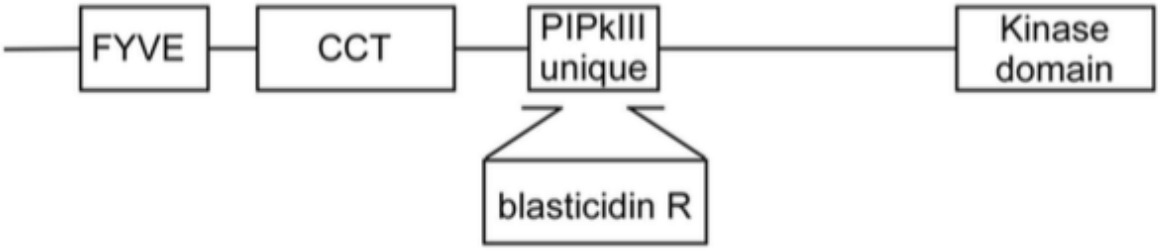

Supplementary figure 1: PIKfyve gene disruption

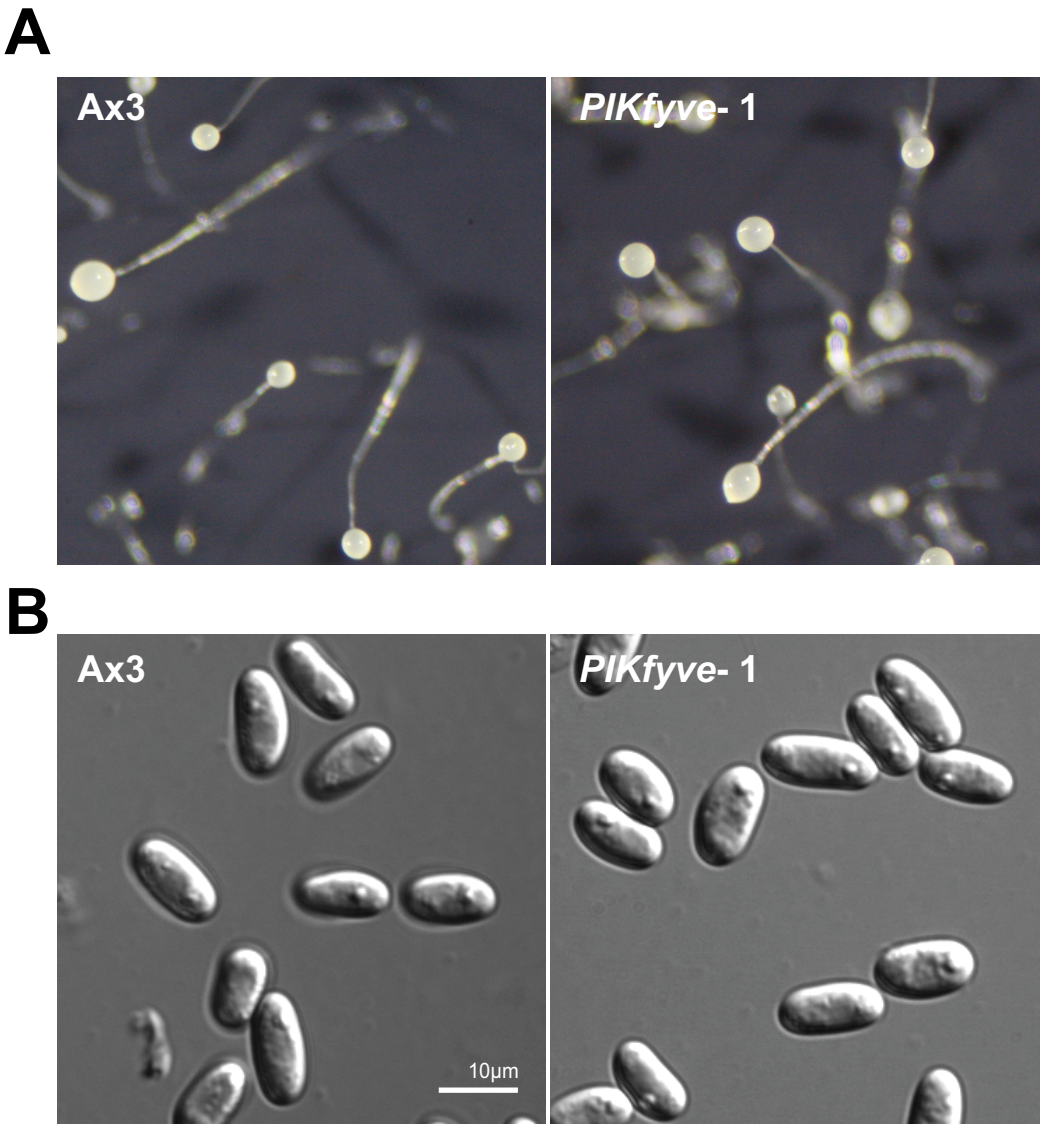

Supplementary figure 2: PIKfyve is not required for development

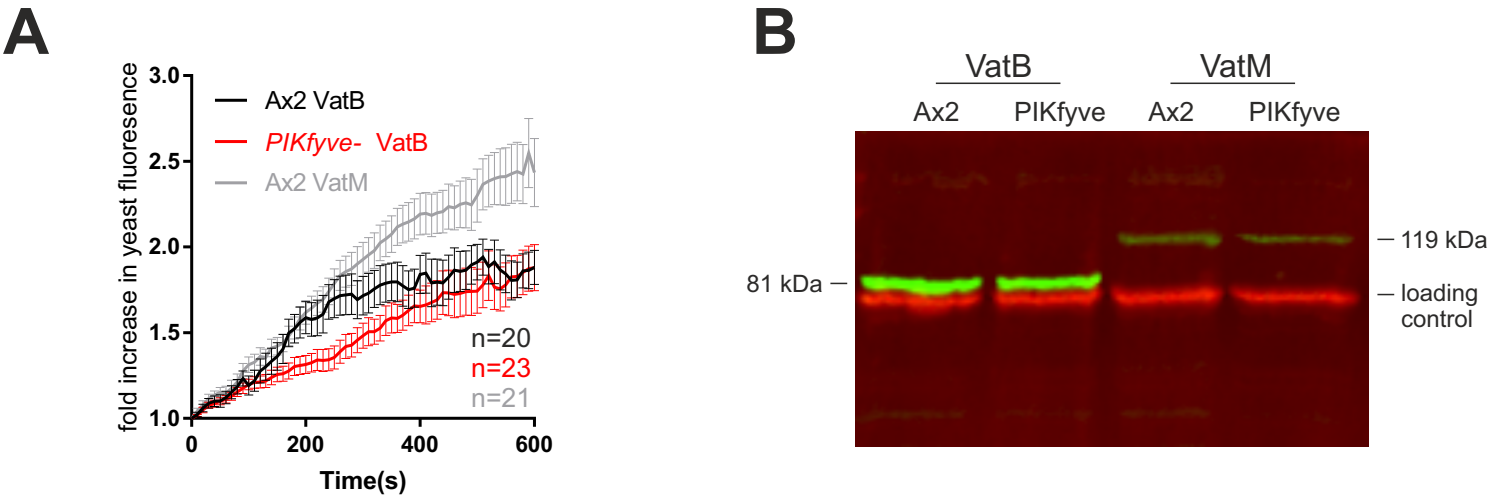

Supplementary figure 3: VatB expression has a dominant negative effect on acidification